Multi-Frequency Radar/Passive Microwave Observations and Simulations of Cold Season Precipitation from GPM and OLYMPEX data

F. Joseph Turk, JPL/Caltech, USA
G. Liu, Florida State Univ., USA
A. Battaglia, F. Tridon, Univ. Leicester, UK

8th International Precipitation Working Group, 3-7 October, Bologna, Italy

Copyright 2016 California Institute of Technology. U.S. government sponsorship acknowledged.

IPWG
International Precipitation Working Group

IWSSM-5
Fifth International Workshop on Space-based Snowfall Measurement

A Merged CloudSat-GPM Coincidence Dataset

F.J. Turk, P. Partain, G. Liu, E. Nelson

±15-minute time coincidences between the GPM and CloudSat ground tracks

Utility includes algorithm evaluation and identification of deficiencies, snow and light rain sensitivity studies, cloud process studies, radiative transfer simulations, surface effects on the radar, radiometer, or combined-sensor precipitation retrieval algorithms, many others….

Current dataset hosted at GSFC-PPS and currently spans the period between 8 March 2014 - 1 December 2015. Of the 5144 coincidences during this time, 2579 had CloudSat data available (I.e., daytime only).

Coincidence files are in HDF5 (10-15 MB each), with three quick-look graphics

Acknowledgments to Erich Stocker (PPS) for hosting these data as a GPM product

https://storm.pps.eosdis.nasa.gov/storm/

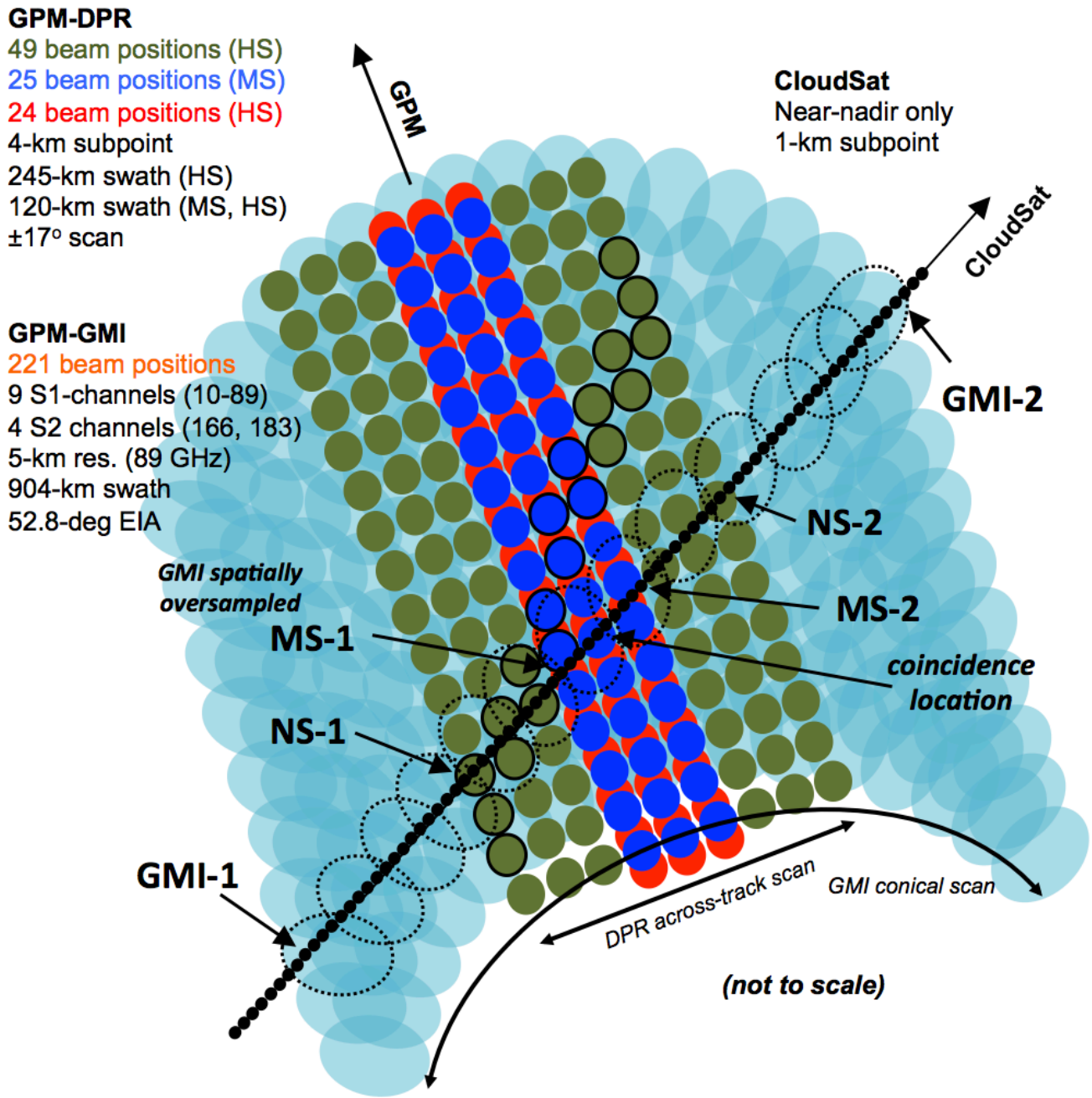
GPM-DPR
49 beam positions (HS)
25 beam positions (MS)
24 beam positions (HS)
4-km subpoint
245-km swath (HS)
120-km swath (MS, HS)
±17° scan
GPM
CloudSat
Near-nadir only
1-km subpoint
CloudSat
GPM-GMI
221 beam positions
9 S1-channels (10-89)
4 S2 channels (166, 183)
5-km res. (89 GHz)
904-km swath
52.8-deg EIA
GMI-2
NS-2
GMI spatially oversampled
MS-2
MS-1
coincidence location
NS-1
GMI-1
DPR across-track scan
GMI conical scan
(not to scale)

245/120-km DPR-Ku/Ka swath

CloudSat subtrack

9 March 2014
01:35:30 - 01:39:16
Near 25S 174W

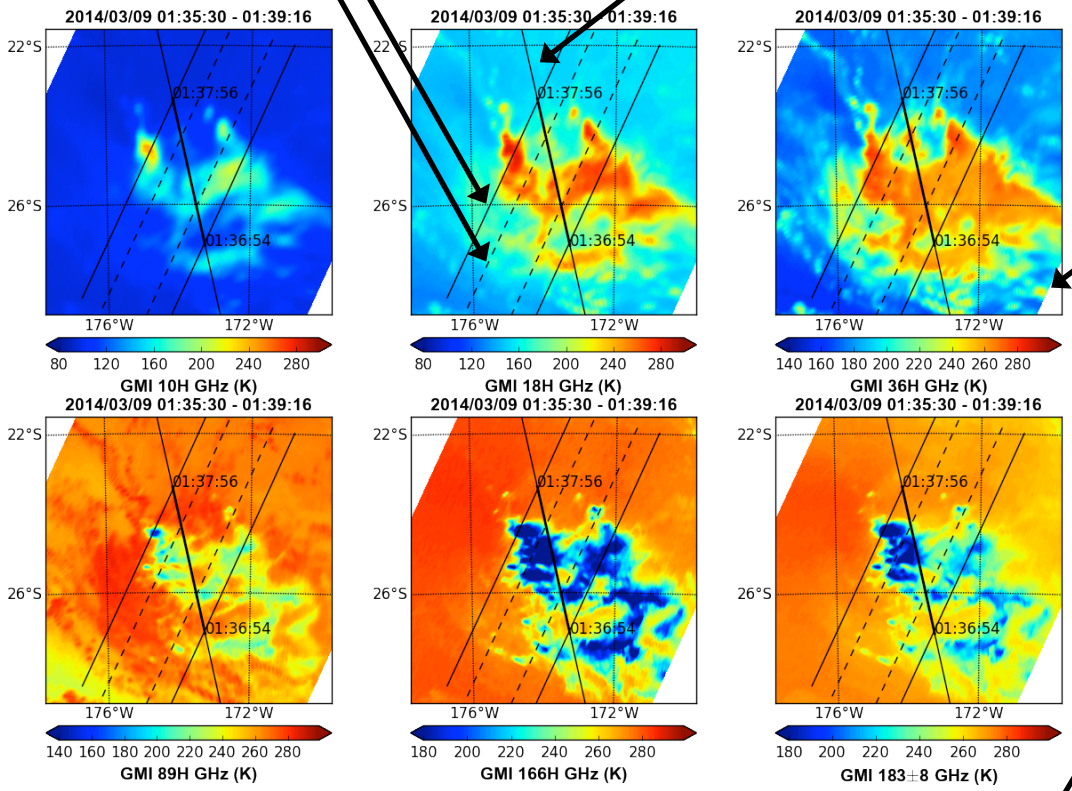

6 of the 13 GMI channels shown
885-km GMI swath

2B-GEOPROF cross section under GMI swath. Trace of 13 TB channels arranged in frequency from top to bottom

10.65V
10.65H
etc...
183.3±7

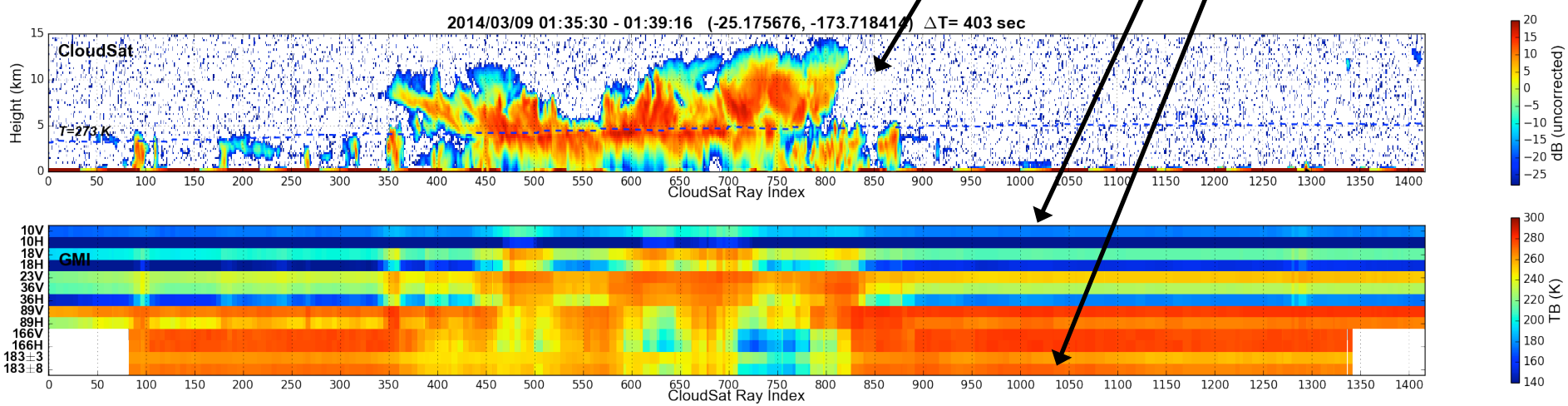

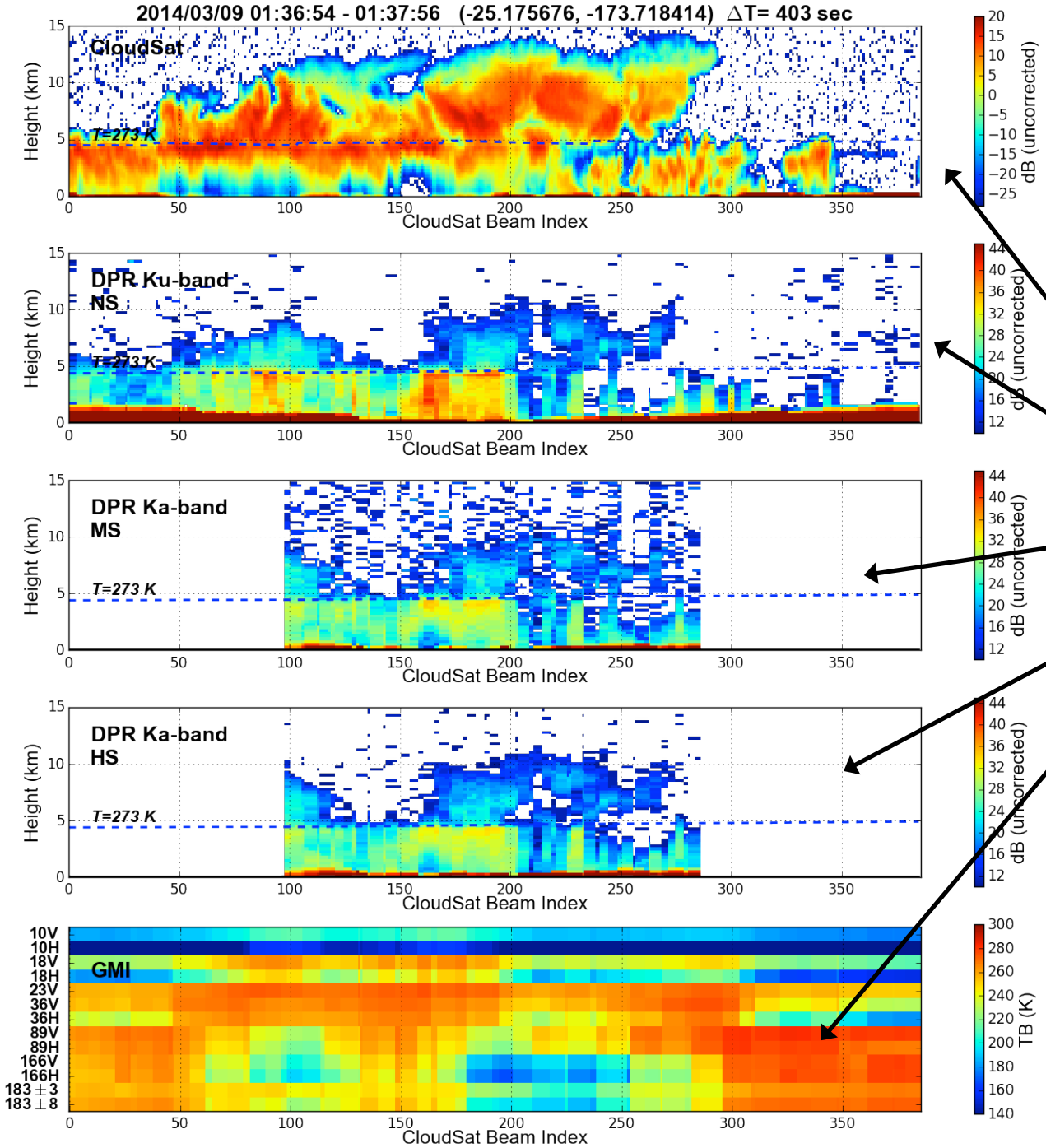

9 March 2014
01:35:30 - 01:39:16
Near 25S 174W

Close-up of subset covering the DPR swath

2B-GEOPROF

DPR-Ku

DPR-Ka

DPR-Ka high sensitivity

Trace of 13 TB channels

APR-3/COSMIR/MASC Analysis from OLYMPEx DC-8 Clear-Sky Flight on 25 November 2015

8 September 2016, PMM Land Surface Group

J. Turk

With acknowledgements to R. Kroodsma (COSMIR), S. Padmanabhan (MASC), T. Lang (AMPR), S. Tanelli, S. Durden, O. Sy (APR-3)

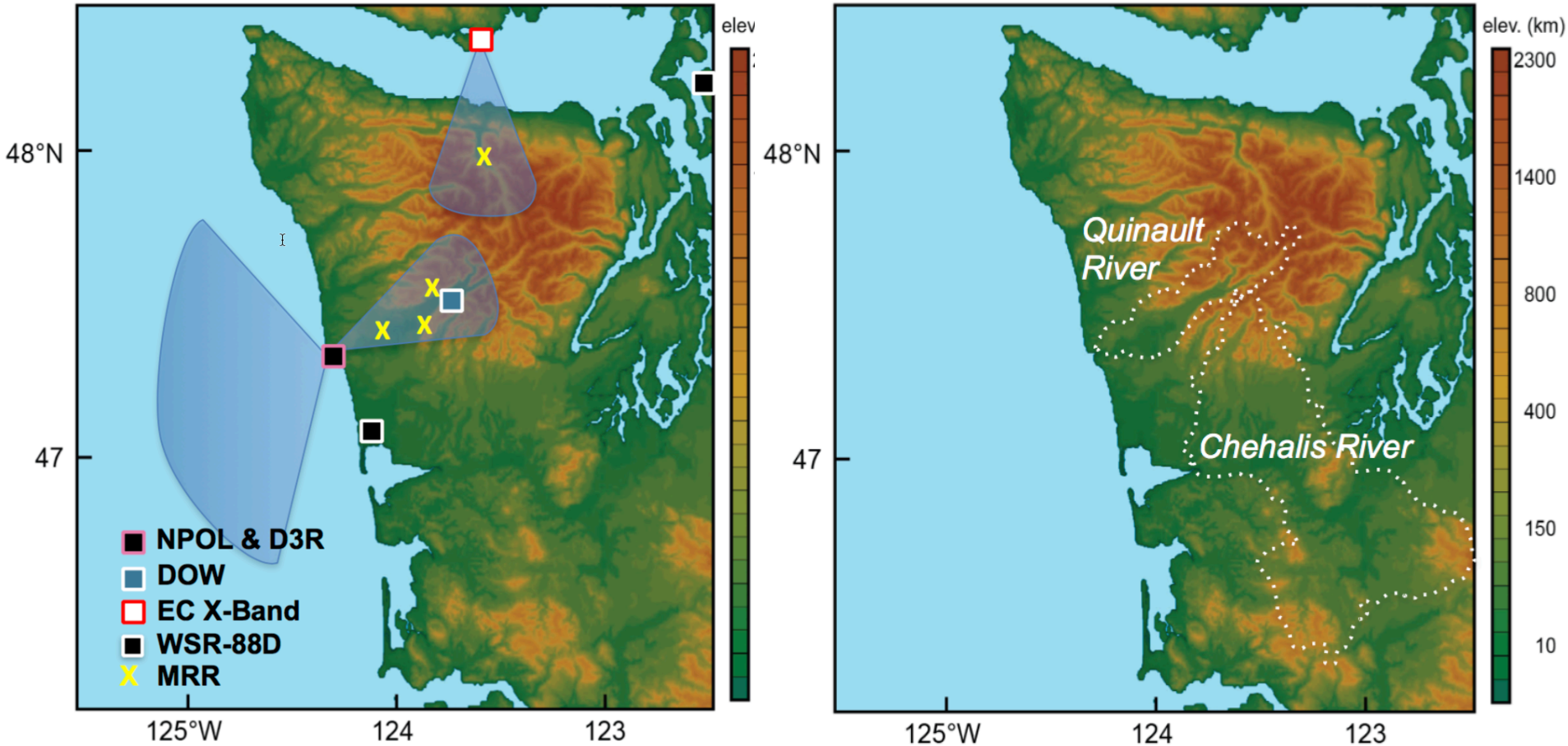

Figure 14: Locations of all the available ground radars for OLYMPEX and the RHI scanning regions for NPOL and EC X-band.

http://olympex.atmos.washington.edu

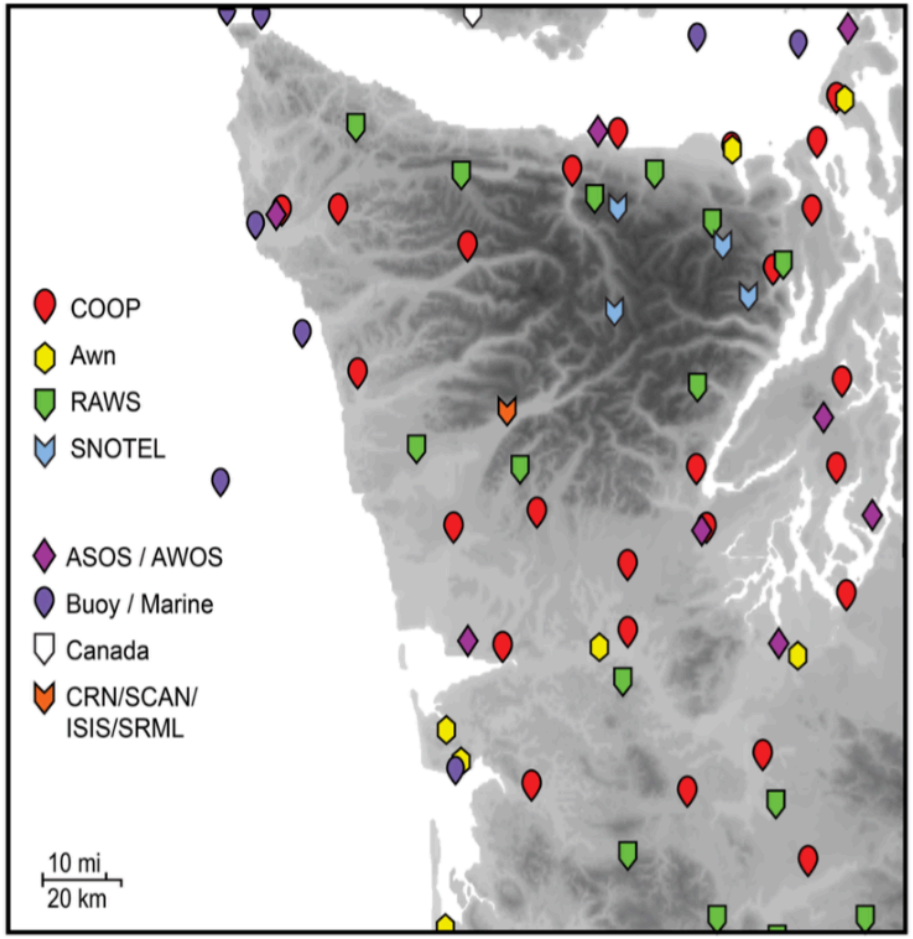

Figure 7: The existing network of surface observations in and around the Olympic Peninsula. ASOS, SNOTEL, RAWS, Buoy, CRN and Canadian sites all report various meteorological parameters hourly, the COOP sites report precipitation once a day.

http://olympex.atmos.washington.edu

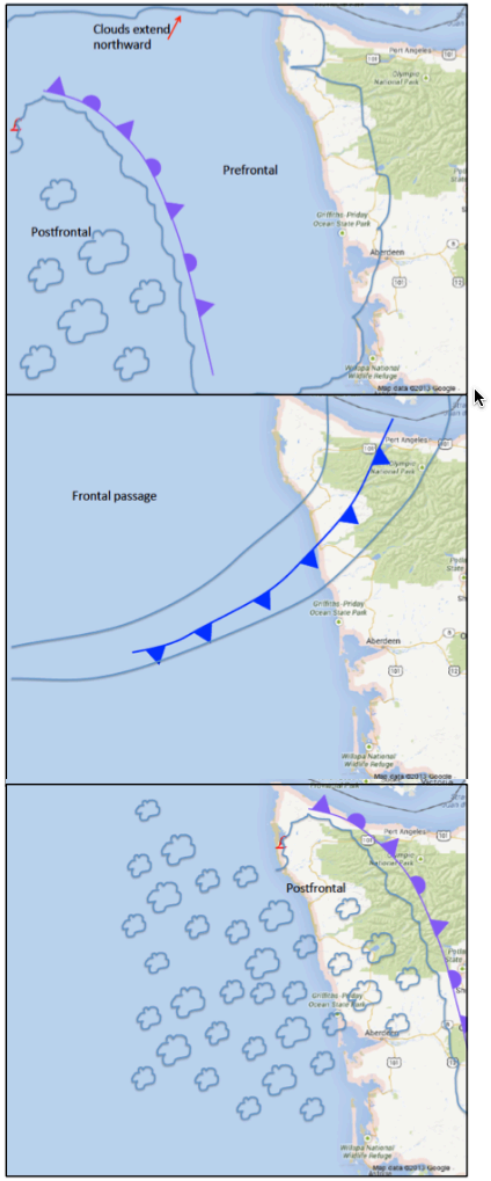

Figure 6: Idealized depiction of the three sectors of a typical midlatitude cyclone. Cloud outlines as seen from satellite imagery shown in blue, standard frontal symbols shown in blue (cold front) and purple (occluded front): Prefrontal (top), Frontal (middle) and Post Frontal (bottom).

DC-8 Instruments

APR-3 (Heritage Ku/Ka-band APR-2, with the added W-band)
9-km swath at 10-km flight altitude

MASC (Microwave Atmospheric Sounder on Cubesat) (8-ch)
183.31±1, 183.31±3, 183.31±7, 183.31±8, 118.75±1, 118.75±2, 118.75±7, 118.75±8

COSMIR (9-ch)
50.3, 52.8, 89V, 89H, 165V, 165H, 183.31±1, 183.31±3, 183.31±7

Dropsondes (over ocean), 3-4 per flight

Many flight segments well-coordinated with ER-2 (not discussed for this time)

APR-3 sigma0 over ocean not shown here

http://olympex.atmos.washington.edu

25 November 2015 Clear-Sky Day No ER-2
Lawn Mower Patterns

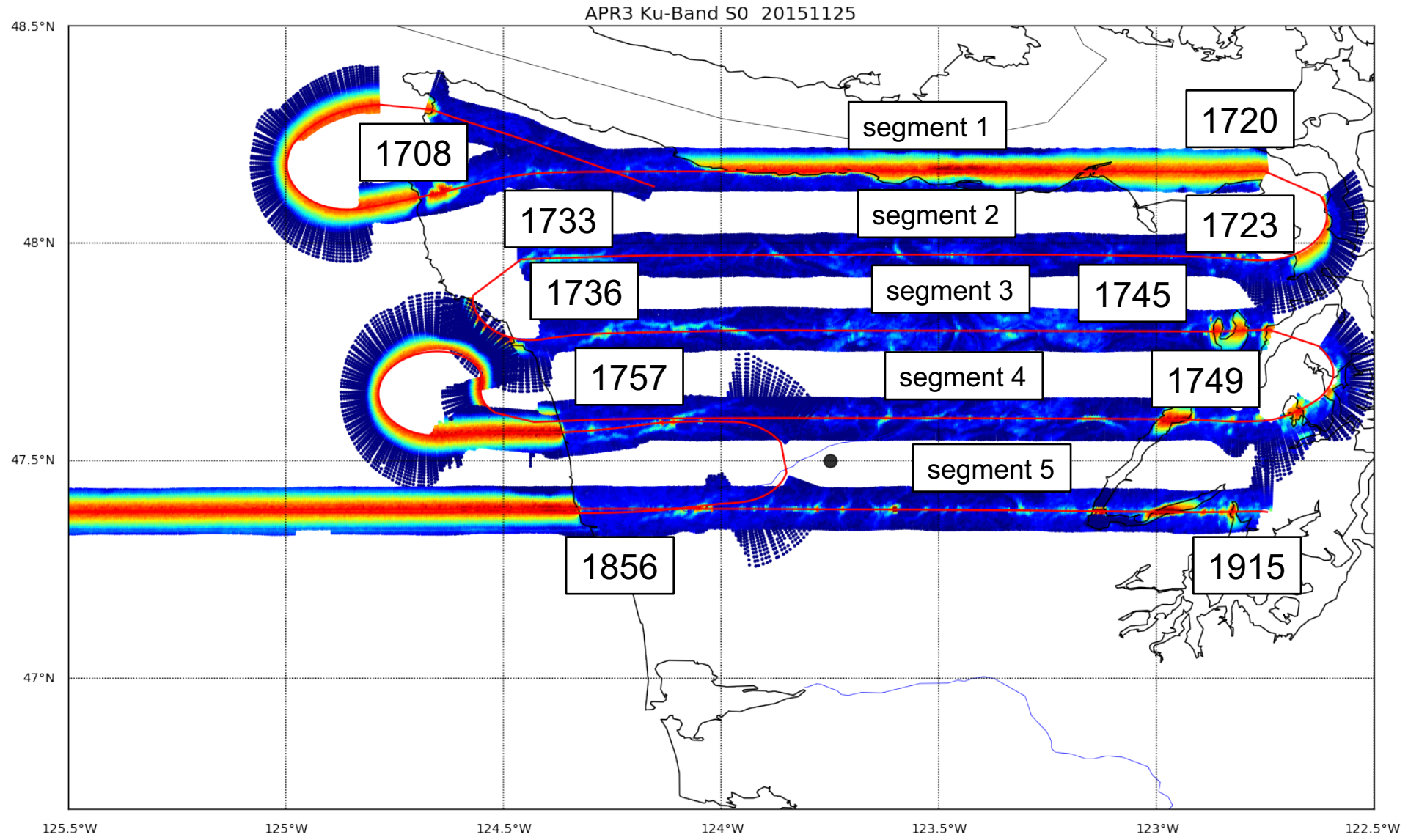
APR3 Ku-Band S0 20151125
48.5°N
48°N
47.5°N
47°N
125.5°W
125°W
124.5°W
124°W
123.5°W
123°W
122.5°W
1708
segment 1
1720
1733
segment 2
1723
1736
segment 3
1745
1757
segment 4
1749
segment 5
1856
1915

COSMIR Forward Simulations Using 1822-1837 UTC Dropsonde

!! very preliminary, nowhere final, still checking absorption in RT code !!

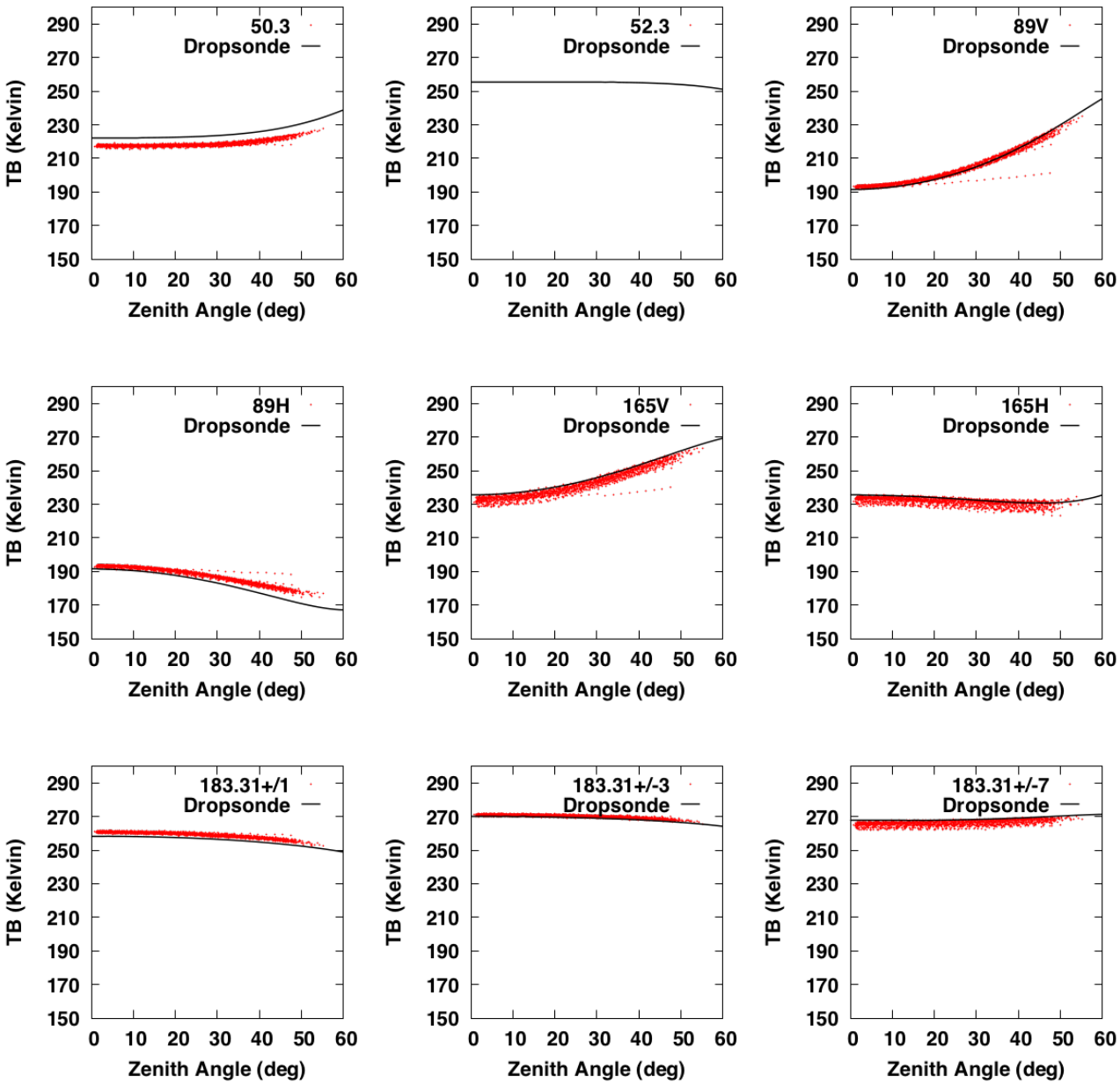

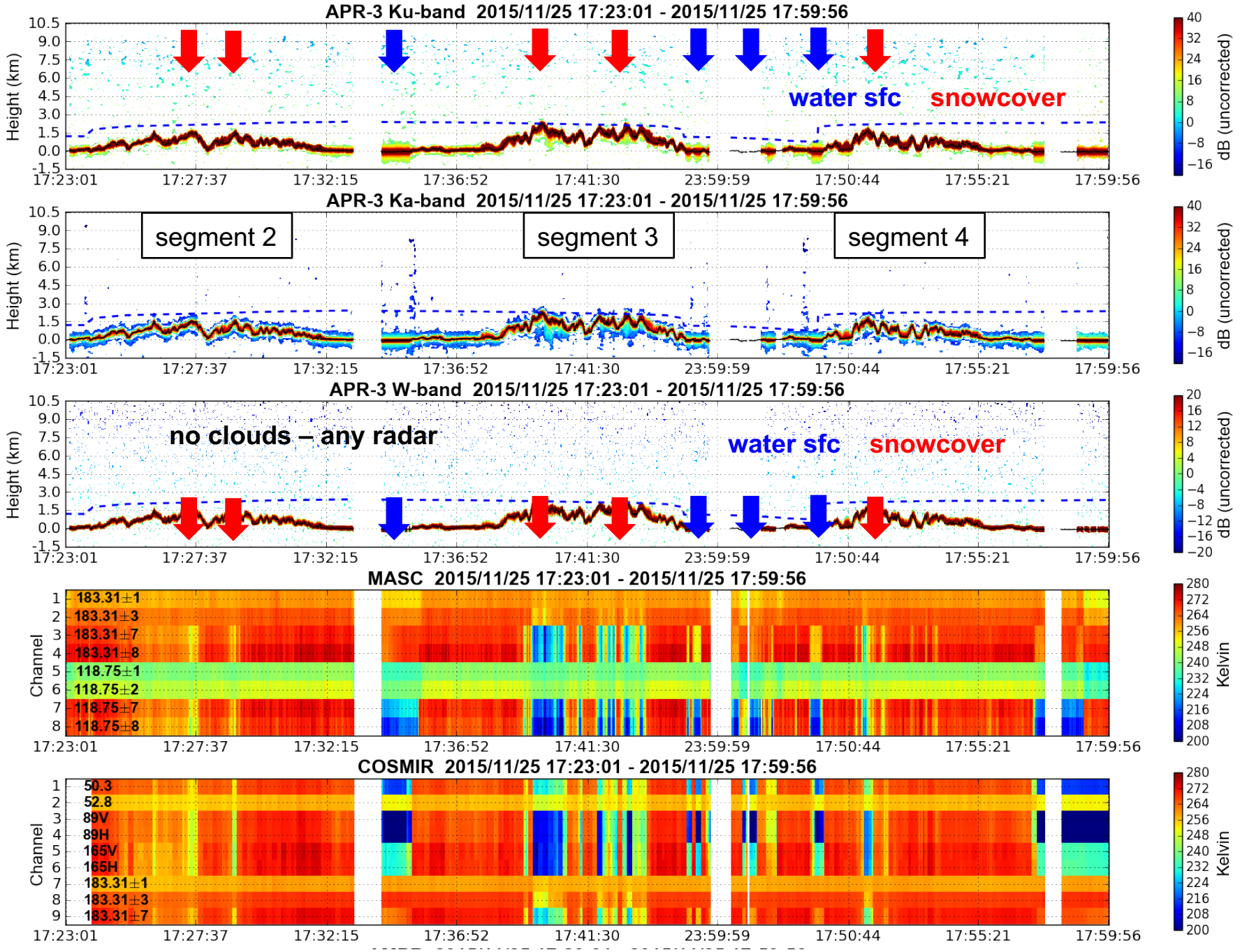
APR-3 Ku-band 2015/11/25 17:23:01 - 2015/11/25 17:59:56
water sfc
snowcover
Height (km)
dB (uncorrected)
APR-3 Ka-band 2015/11/25 17:23:01 - 2015/11/25 17:59:56
segment 2
segment 3
segment 4
APR-3 W-band 2015/11/25 17:23:01 - 2015/11/25 17:59:56
no clouds – any radar
MASC 2015/11/25 17:23:01 - 2015/11/25 17:59:56
183.31±1
183.31±3
183.31±7
183.31±8
118.75±1
118.75±2
118.75±7
118.75±8
Channel
Kelvin
COSMIR 2015/11/25 17:23:01 - 2015/11/25 17:59:56
50.3
52.8
89V
89H
165V
165H
183.31±1
183.31±3
183.31±7
17:23:01
17:27:37
17:32:15
17:36:52
17:41:30
23:59:59
17:50:44
17:55:21
17:59:56

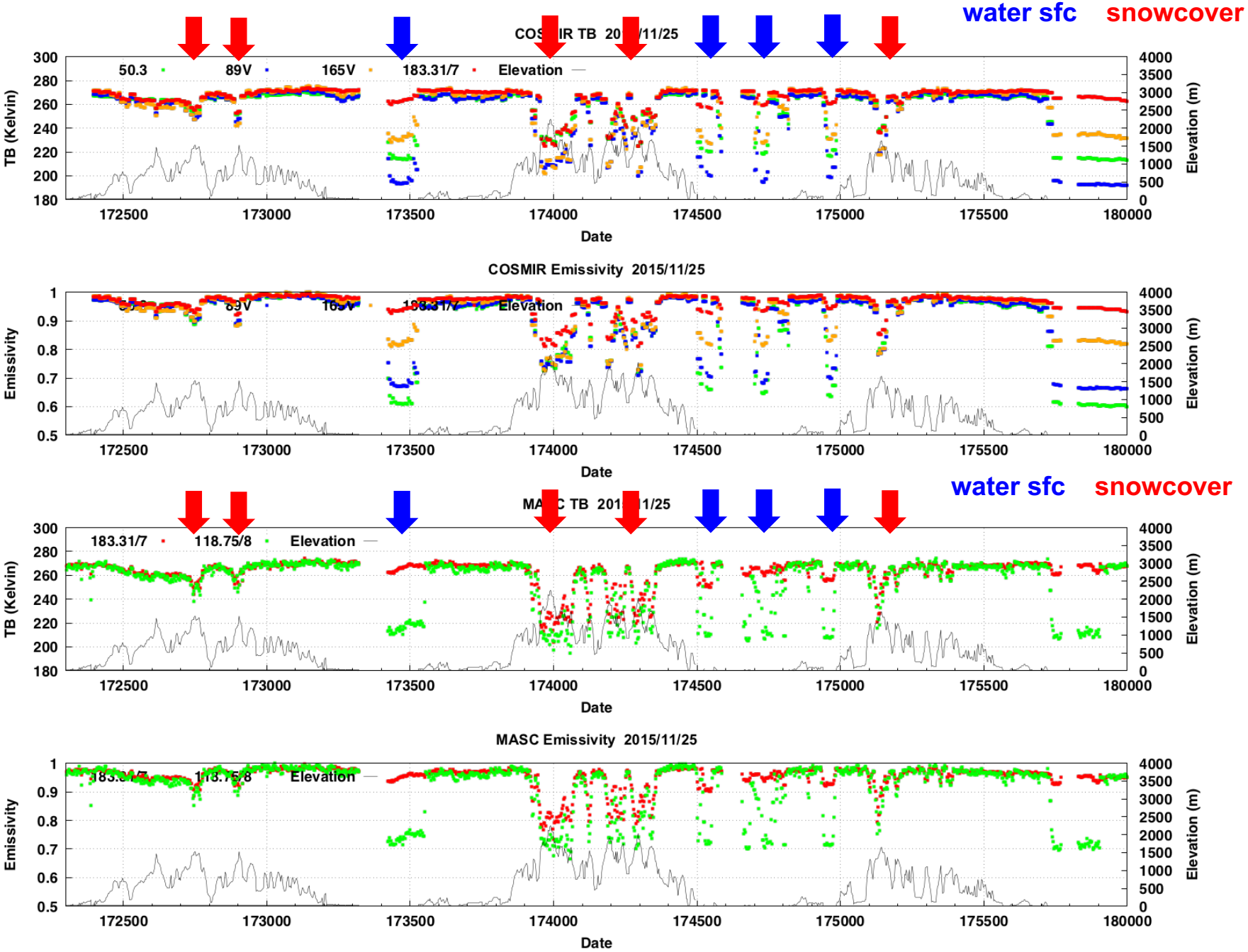
water sfc
snowcover
COSMIR TB 2015/11/25
50.3
89V
165V
183.31/7
Elevation
TB (Kelvin)
Elevation (m)
Date
COSMIR Emissivity 2015/11/25
Emissivity
MASC TB 2015/11/25
118.75/8
MASC Emissivity 2015/11/25

Six Days Later: 1 December 2015 With ER-2

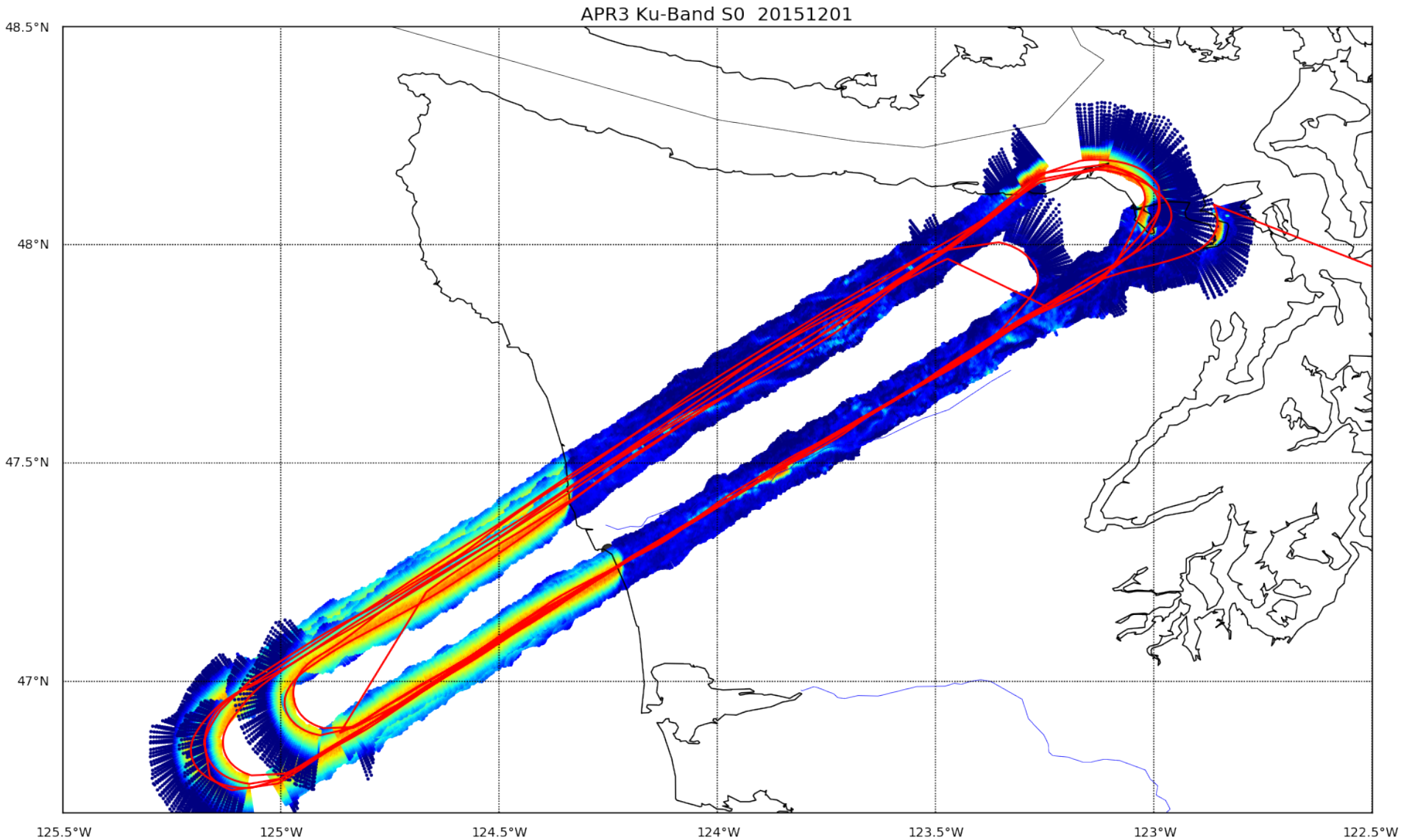

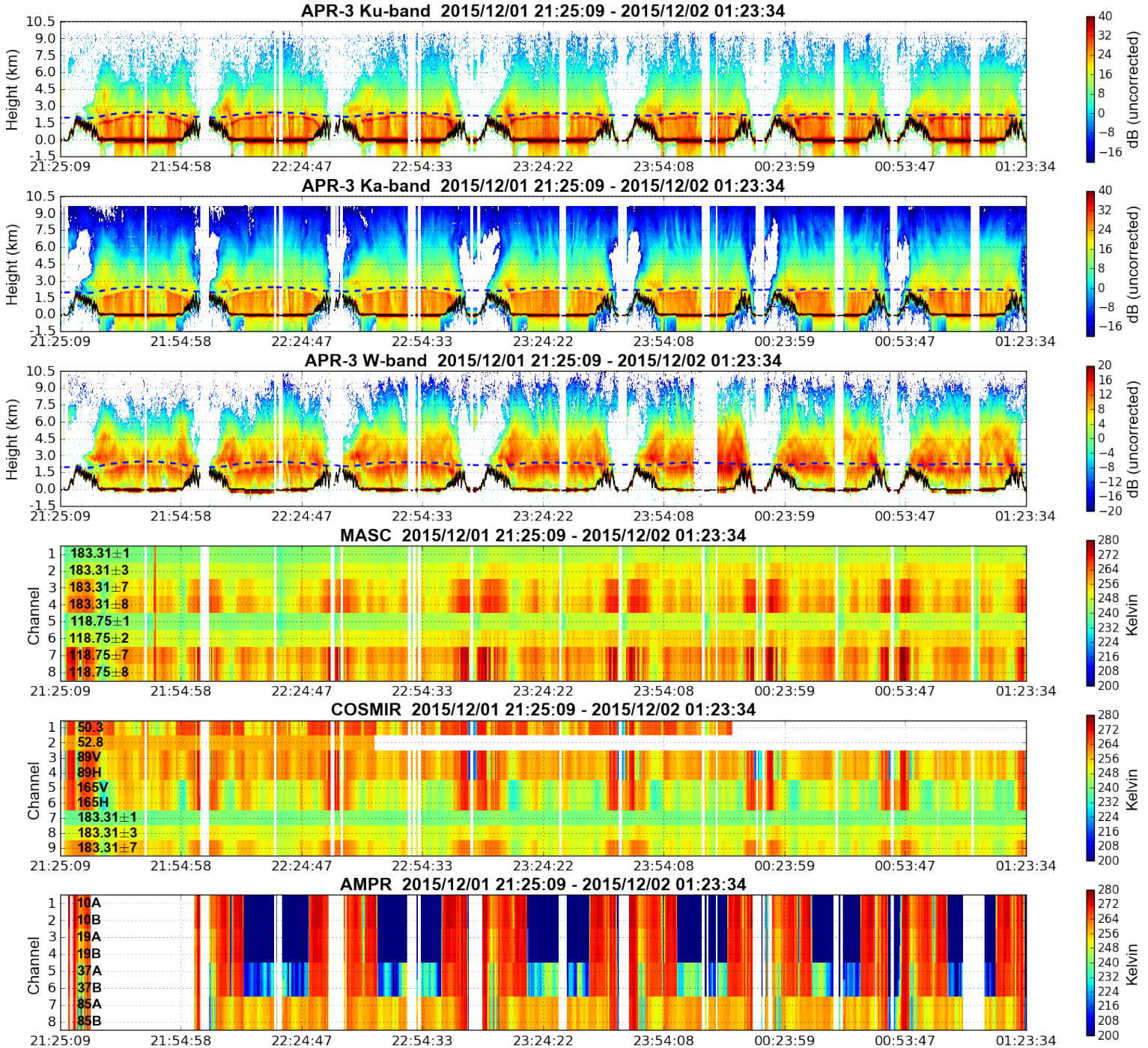
APR-3 Ku-band 2015/12/01 21:25:09 - 2015/12/02 01:23:34
Height (km)
dB (uncorrected)
APR-3 Ka-band 2015/12/01 21:25:09 - 2015/12/02 01:23:34
Height (km)
dB (uncorrected)
APR-3 W-band 2015/12/01 21:25:09 - 2015/12/02 01:23:34
Height (km)
dB (uncorrected)
MASC 2015/12/01 21:25:09 - 2015/12/02 01:23:34
Channel
183.31±1
183.31±3
183.31±7
183.31±8
118.75±1
118.75±2
118.75±7
118.75±8
Kelvin
COSMIR 2015/12/01 21:25:09 - 2015/12/02 01:23:34
Channel
50.3
52.8
89V
89H
165V
165H
183.31±1
183.31±3
183.31±7
Kelvin
AMPR 2015/12/01 21:25:09 - 2015/12/02 01:23:34
Channel
10A
10B
19A
19B
37A
37B
85A
85B
Kelvin
21:25:09
21:54:58
22:24:47
22:54:33
23:24:22
23:54:08
00:23:59
00:53:47
01:23:34

All APR-3 Flight Tracks (red) During OLYMPEX (Ku-band s0 in color)

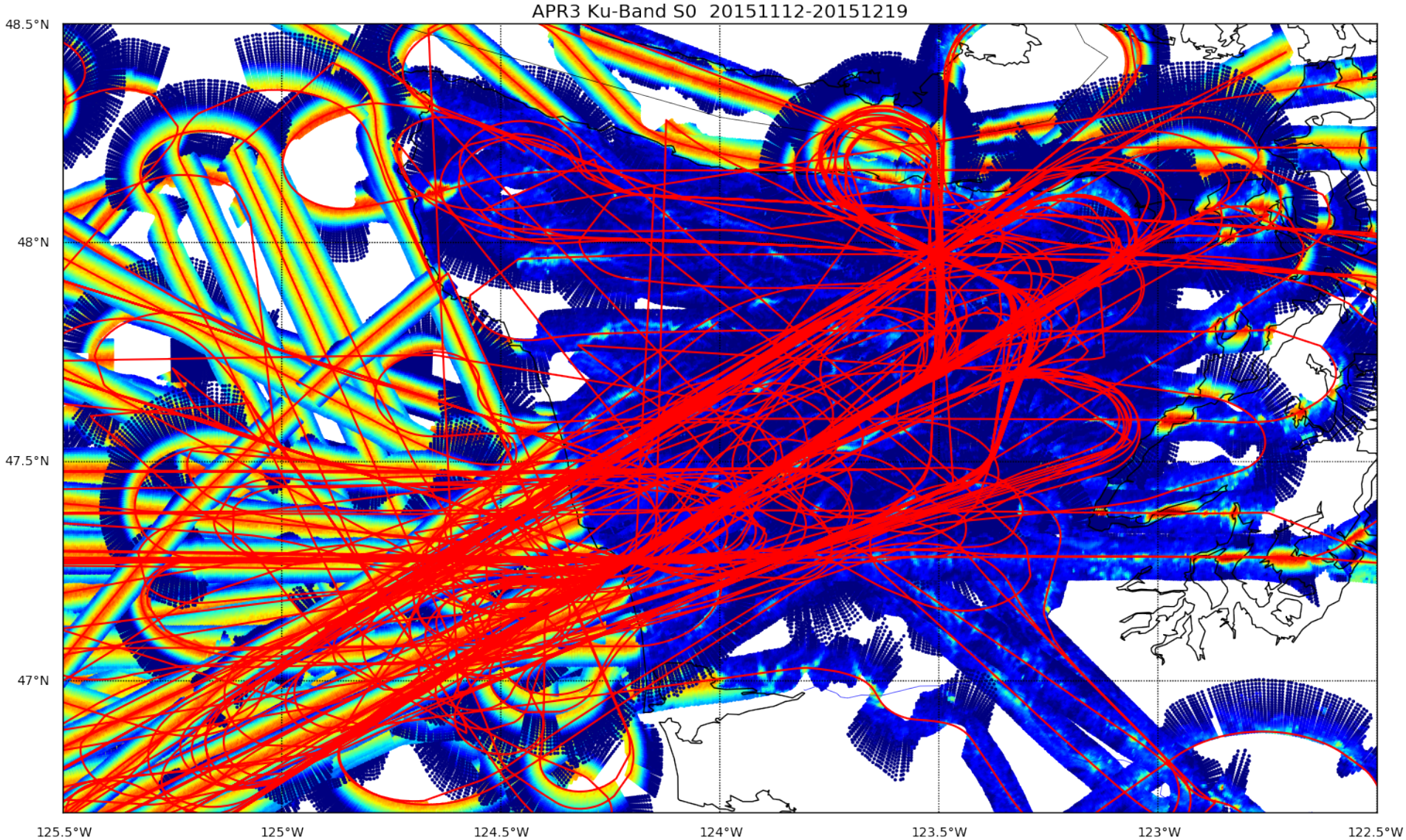

Preliminary Analysis of Land Surface Backscatter from OLYMPEX
Joe Turk, JPL

APR3 data were only used when the column Zmax14 and Zmax35 < 20 dB (crude no-precip screen)

The APR3 zenith angle is the incidence angle that each APR3 beam makes with the surface. Since the DC-8 often banked rather tightly during OLYMPEX, this angle can exceed 60 degrees, but it never gets much below 3-degrees given the radar mounting and the typical aircraft pitch. I only show up to 17-degrees to match with DPR.

The boxplots show 10, 25, 50, 75, 90 percent quintiles each angle bin

DPR data were taken during Nov-Dec 2015 for comparison, within the domain 46.9-48.5 latitude, -125.2 to -122.7 longitude region (1.5 deg x 2.5 degree box). Data with either the NS and MS precip flags set were excluded.

A common land/ocean mask was used for APR3 and DPR. The mask is coarse (0.05 minute resolution) and coastal regions were excluded. This allows the same land/ocean mask for each sensor, and forces the analysis to cover (almost) the same Earth surface locations.

APR-3

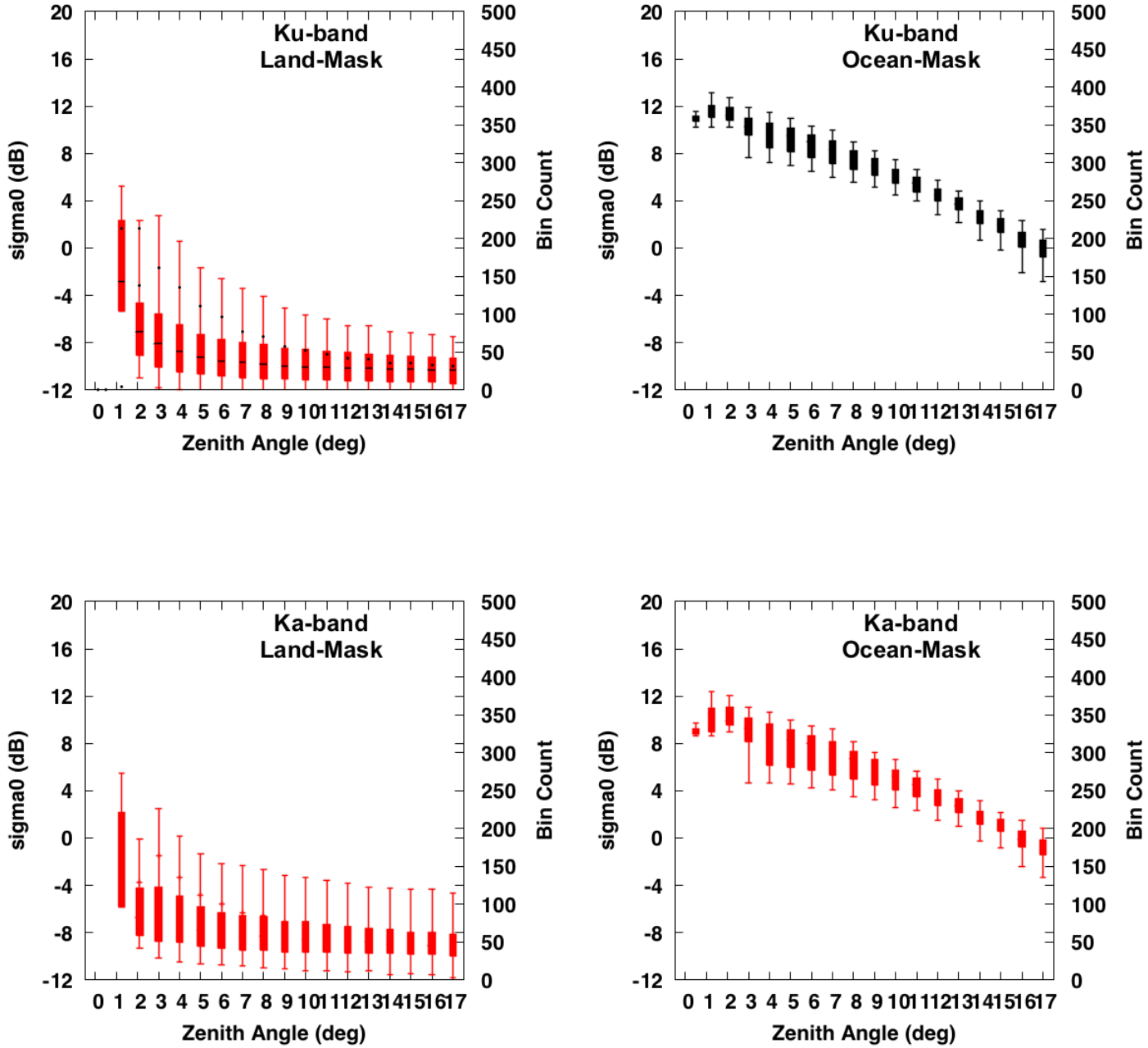
Ku-band
Land-Mask
Ku-band
Ocean-Mask
Ka-band
Land-Mask
Ka-band
Ocean-Mask
sigma0 (dB)
Bin Count
Zenith Angle (deg)
20
16
12
8
4
0
-4
-8
-12
500
450
400
350
300
250
200
150
100
50
0
0 1 2 3 4 5 6 7 8 9 10 11 12 13 14 15 16 17

DPR

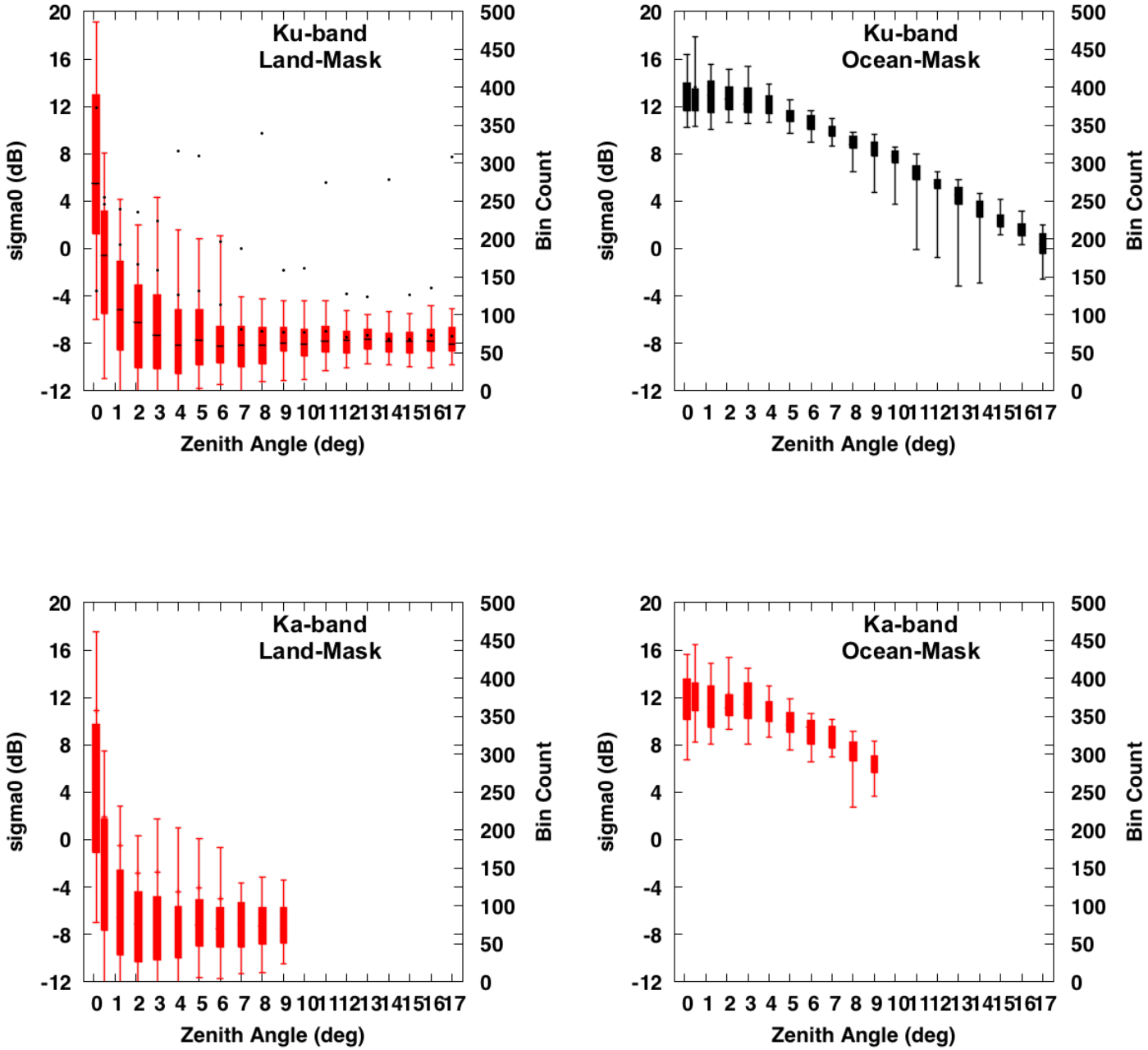
Ku-band
Land-Mask
Ku-band
Ocean-Mask
Ka-band
Land-Mask
Ka-band
Ocean-Mask
sigma0 (dB)
Bin Count
Zenith Angle (deg)
20
16
12
8
4
0
-4
-8
-12
500
450
400
350
300
250
200
150
100
50
0
0 1 2 3 4 5 6 7 8 9 10 11 12 13 14 15 16 17

Why is this work needed?

- The information content within space-based precipitation radar/radiometer observations is insufficient to describe the environmental and surface state controlling the precipitation process physics.

- Retrieval process brings in a-priori simulations and ancillary data, in order to apply common physics across all platforms/sensors. Places a heavy burden on the "realism" of the Z and TB simulations.

- For simulations the MW surface emissivity vector needs to be specified for each sensor type, alongside associated thermodynamic state.

- And for retrievals, some way of "connecting" to the properties used for creating each database profile

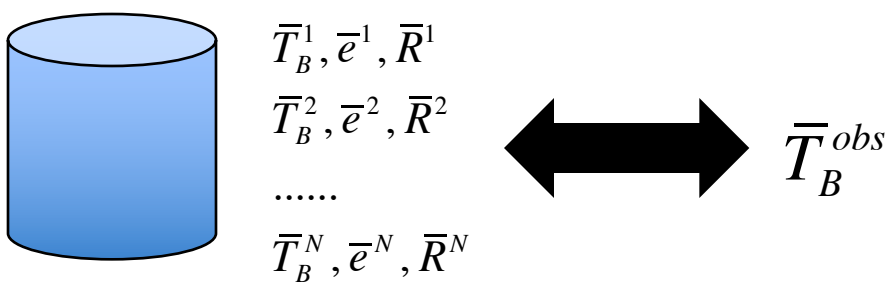

A-priori ***Observations***

"connect" surface and environmental conditions to corresponding conditions within the a-priori collection

Current GPM-GPROF does this thru a "classification index"

(Figure courtesy of Dr. Wes Berg, Colorado State Univ.)

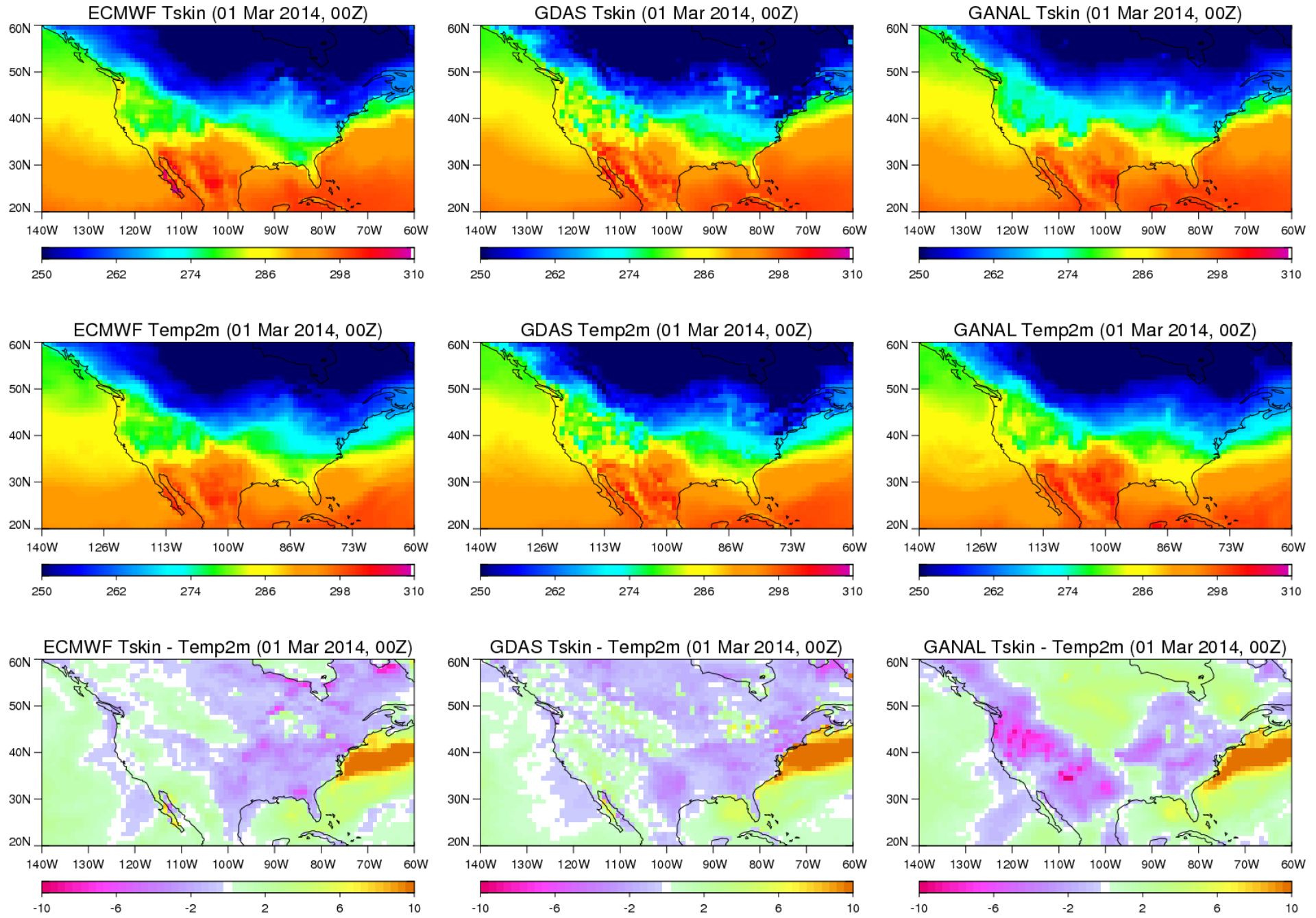

Using DPR for Radiometer Scene Discrimination

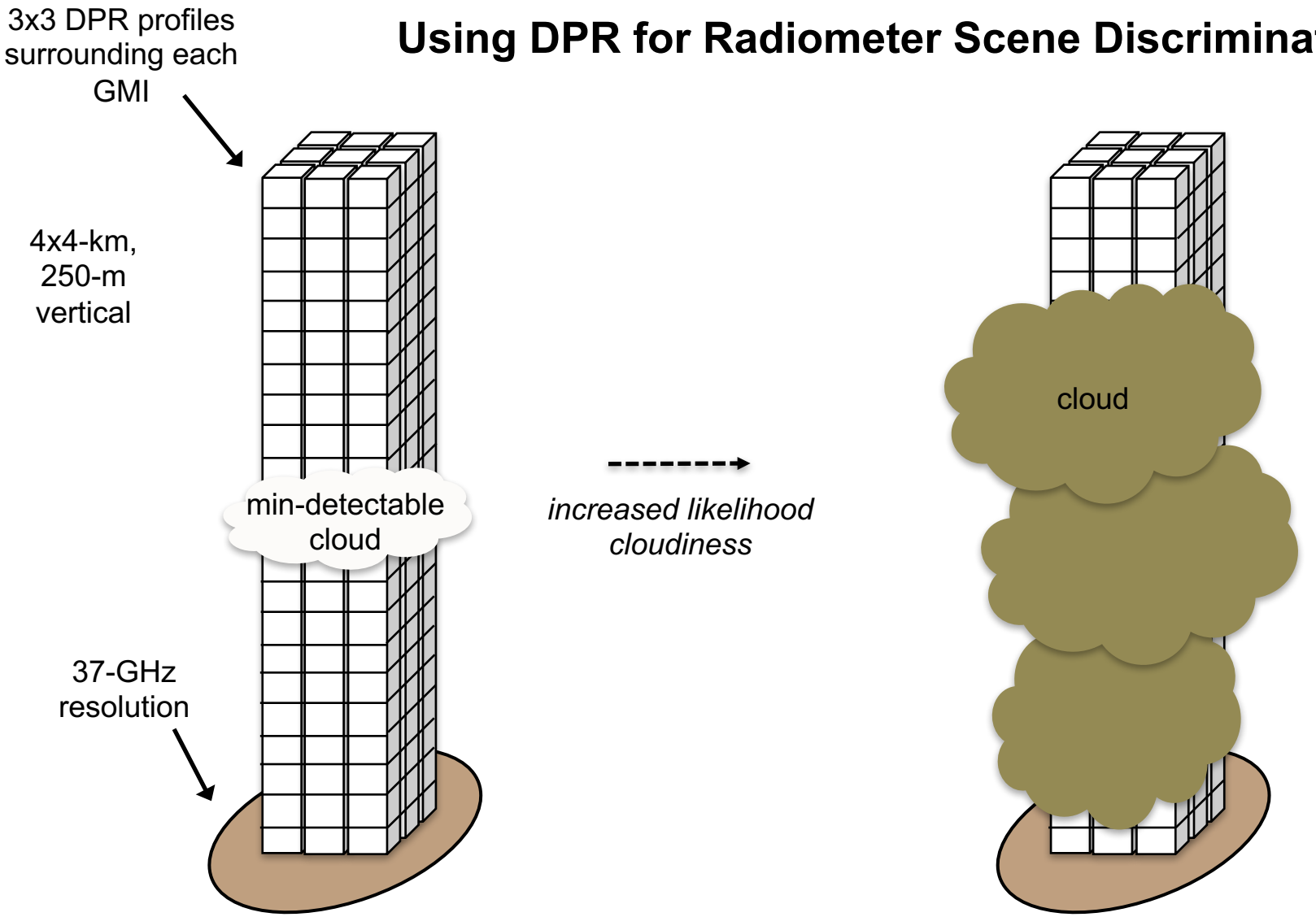

Z(Ku) < 15 dB and
Z(Ka) < 15 dB and
Z(Ka-HS) < 15 dB
(all bins) ➔ "no cloud"

N bins where Z(Ku) > 20 dB as a proxy for increased level of cloudiness and precipitation

N > 20 ➔ "low probability"
N > 50 ➔ "medium probability"
N > 100 ➔ "high probability"

Analysis Matched GMI/DPR Data

Extensive, diverse collection from 1+ year of GMI "no-cloud" emissivity vectors everywhere within ±65 degree latitude, without regard to the surface type

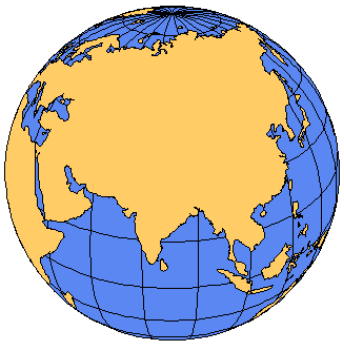

$$\begin{bmatrix} TB_{10V} \\ TB_{10H} \\ \cdots \\ TB_{89H} \\ TB_{166V} \\ TB_{166H} \end{bmatrix} + \begin{bmatrix} e_{10V} \\ e_{10H} \\ \cdots \\ e_{89H} \\ T_{sfc} \\ TWV \end{bmatrix}$$

Tsfc and total vapor added

Principal component analysis :

$$\vec{u} = \left[E\right]^T \vec{e}$$

$$\left[\Lambda\right] = \left[E\right]^{-1} \left[S_x\right] \left[E\right]$$

$$\vec{e} \equiv \left[E\right] \vec{u}$$

$$\vec{e} \cong \left[E\right] \hat{u}$$

If there was some way to estimate each principal component from the observations, then the emissivity vector e could be *approximately* reconstructed from the TB observations

Assume nonlinear TB combinations and polarization ratios "carry" the information on the surface properties

$$u_i = a_0 + \sum_{j=1}^{N} a_j TB_j + \sum_{j=1}^{N} \sum_{k=j}^{N} b_{jk} TB_j TB_k + \sum_{j=1}^{3} c_j PR_j \qquad i = 1,9$$

$$PR_j = (TB_j^V - TB_j^H) / (TB_j^V + TB_j^H) \qquad j = 1,3$$

TB-Reconstructed Emissivity State Vector

N=9 (10-89 GHz)
High water vapor over land underestimated

N=11 (10-166 GHz)
Improvement in over-land total vapor with inclusion of 166 GHz channels

N=7 (19-85 GHz SSMIS)
SSMIS (no 10 GHz) dataset from 1-year of F17-GPM 15-min coincidences

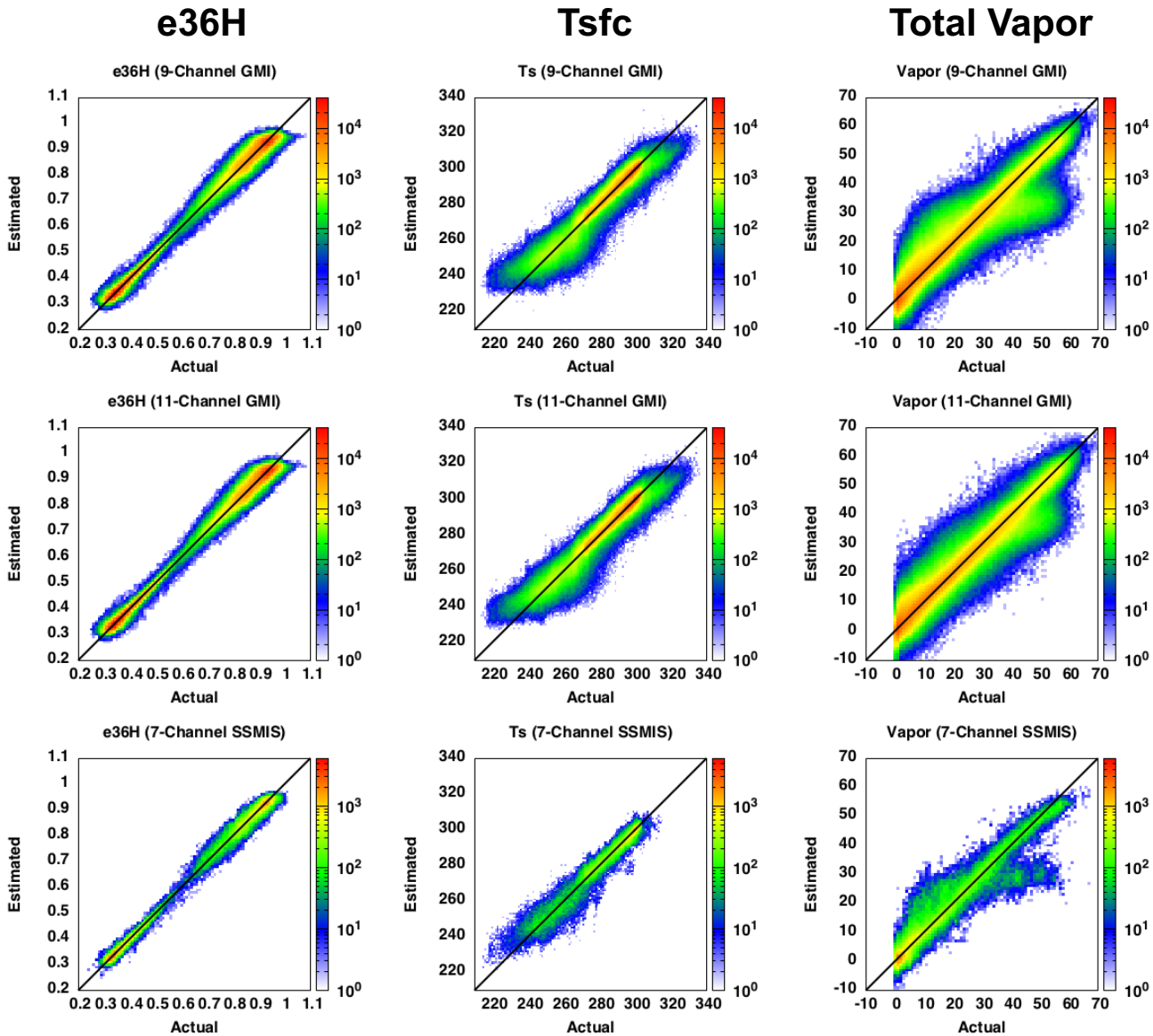

Discrimination Performance
N(Ku) > 20 dB in column
N>0 N>20 N>50 N>100

3 PC-based discriminant, using 9-channels in the regression, is a good compromise, also since S2 (166, 183 GHz) channels not always available

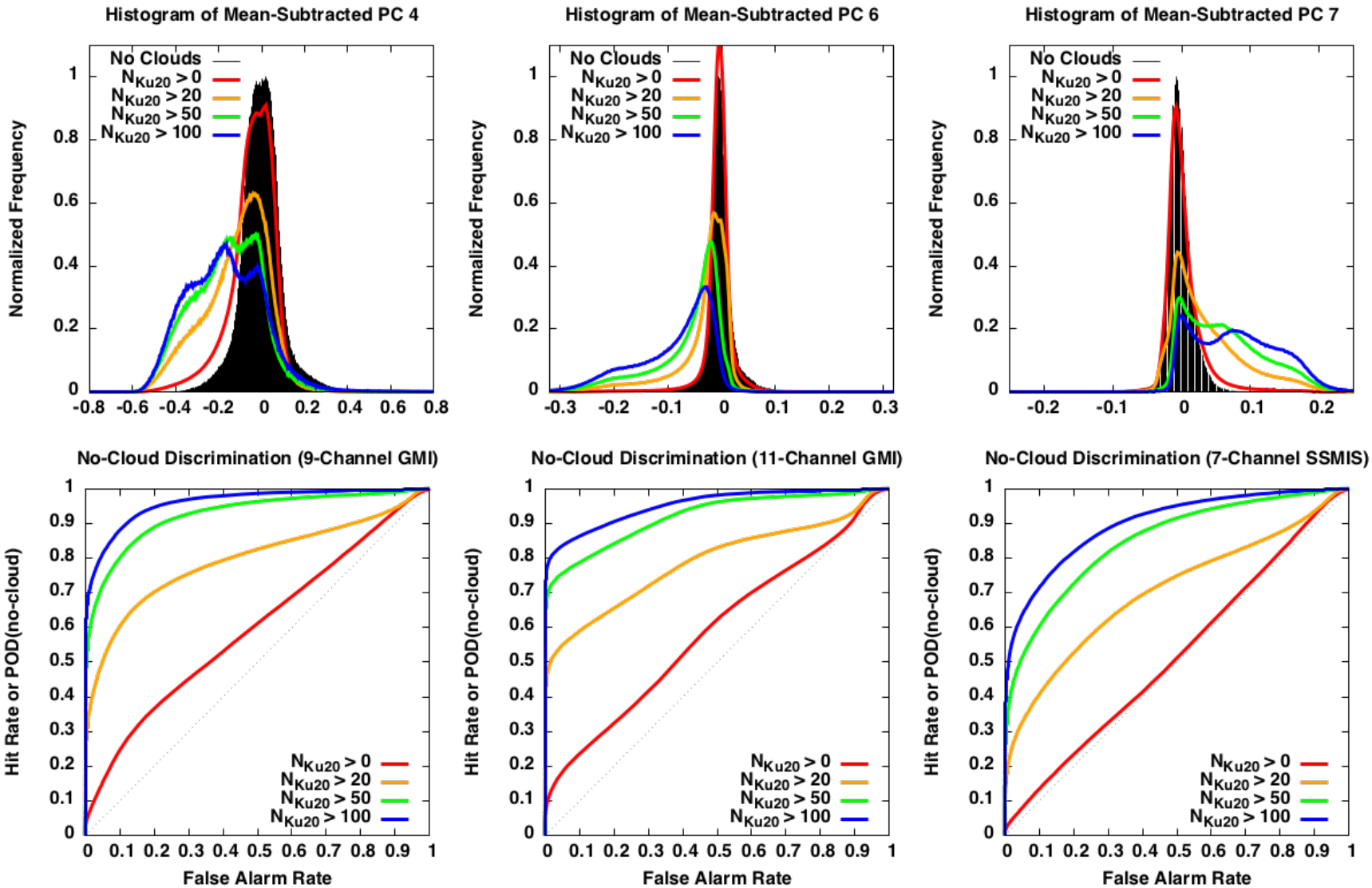

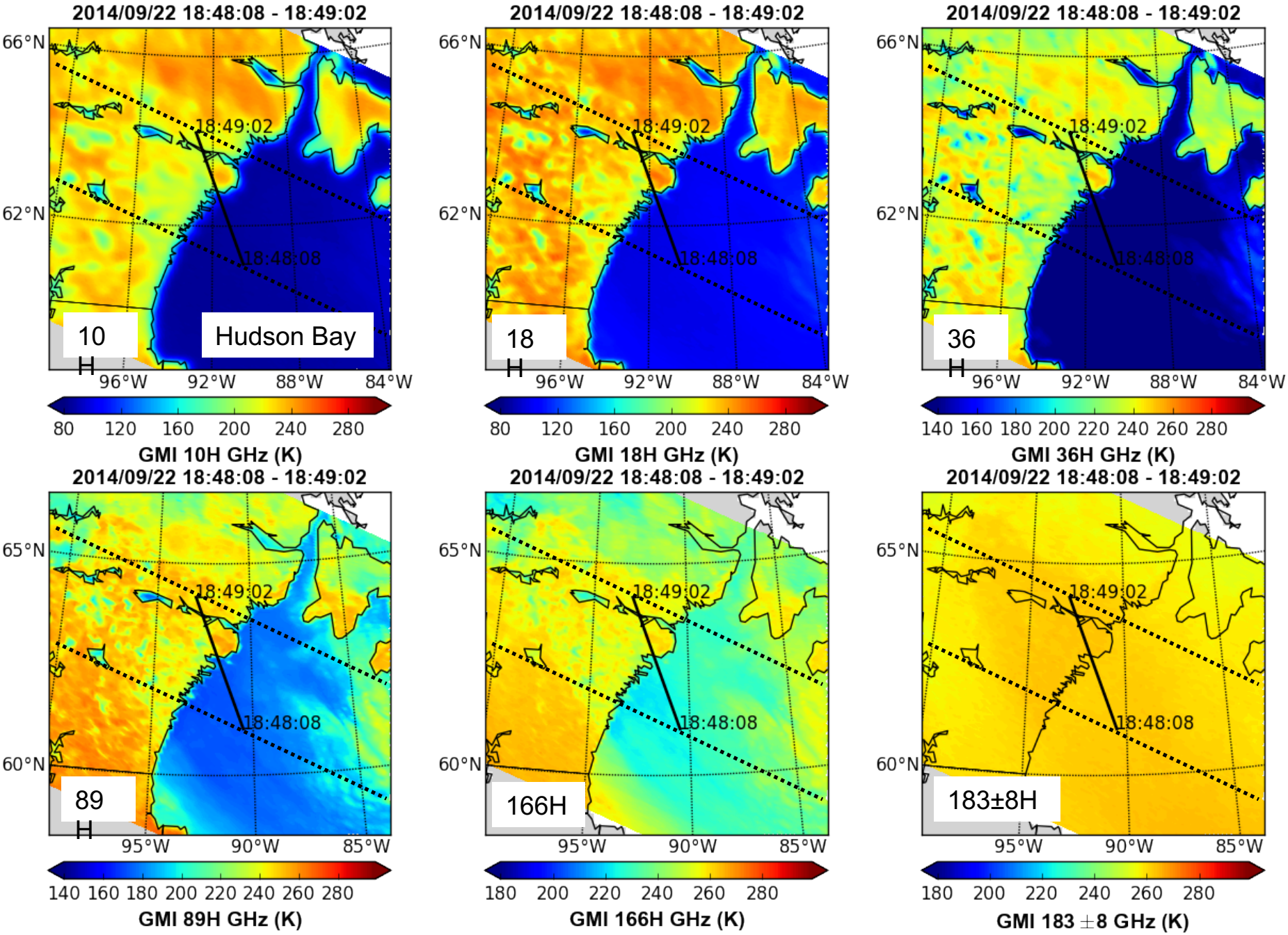
2014/09/22 18:48:08 - 18:49:02
66°N
62°N
18:49:02
18:48:08
10 H
Hudson Bay
96°W
92°W
88°W
84°W
80 120 160 200 240 280
GMI 10H GHz (K)
2014/09/22 18:48:08 - 18:49:02
66°N
62°N
18:49:02
18:48:08
18 H
96°W
92°W
88°W
84°W
80 120 160 200 240 280
GMI 18H GHz (K)
2014/09/22 18:48:08 - 18:49:02
66°N
62°N
18:49:02
18:48:08
36 H
96°W
92°W
88°W
84°W
140 160 180 200 220 240 260 280
GMI 36H GHz (K)
2014/09/22 18:48:08 - 18:49:02
65°N
60°N
18:49:02
18:48:08
89 H
95°W
90°W
85°W
140 160 180 200 220 240 260 280
GMI 89H GHz (K)
2014/09/22 18:48:08 - 18:49:02
65°N
60°N
18:49:02
18:48:08
166H
95°W
90°W
85°W
180 200 220 240 260 280
GMI 166H GHz (K)
2014/09/22 18:48:08 - 18:49:02
65°N
60°N
18:49:02
18:48:08
183±8H
95°W
90°W
85°W
180 200 220 240 260 280
GMI 183 ±8 GHz (K)

GPM+CloudSat Coincidence
22 September 2014
Hudson Bay Land-Water

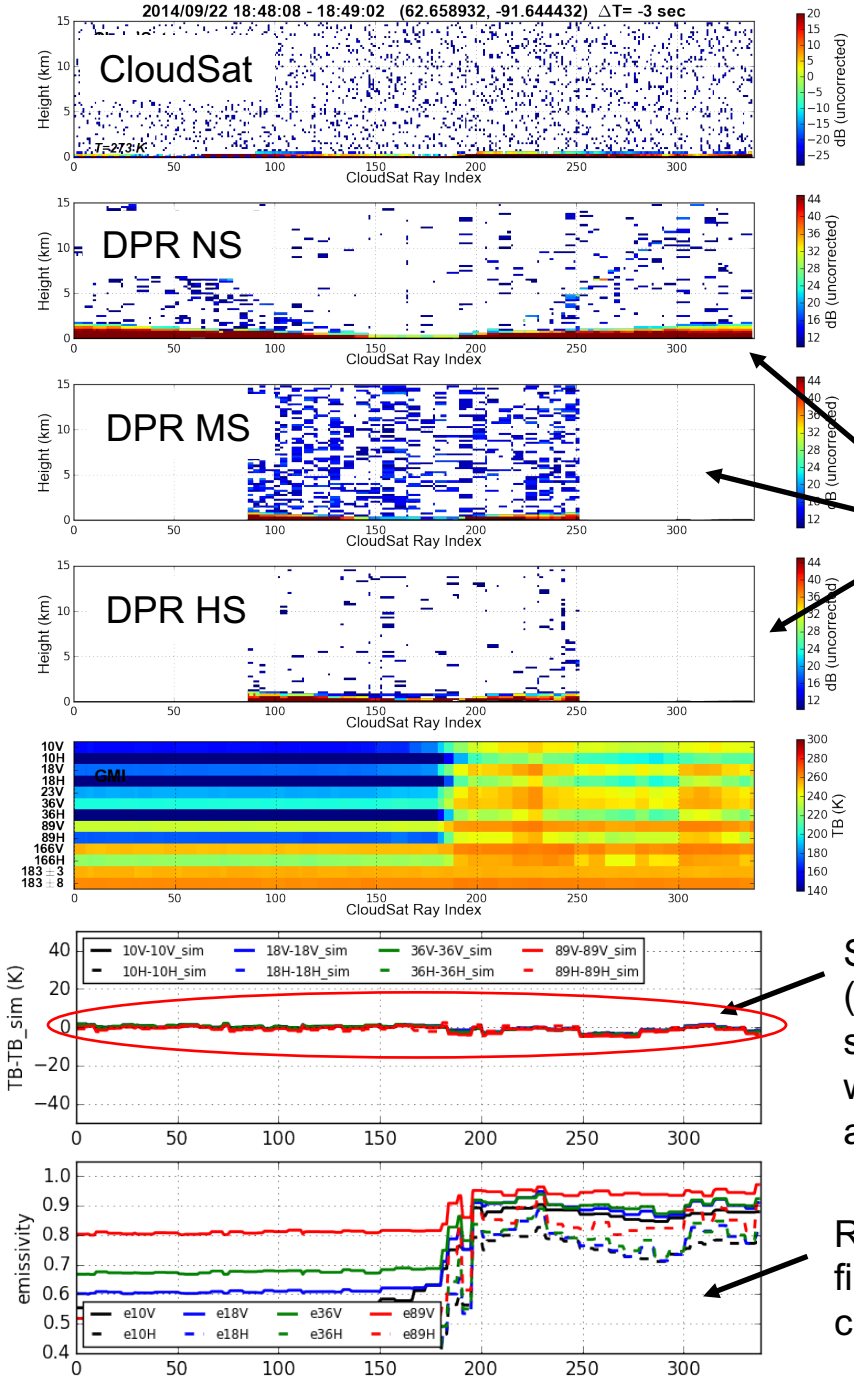

No clouds evident in all three DPR scans

Trace of all 13 GMI channels

Simulated TB difference (using ECMWF) Near seamless land-coast-water transition across all 9 GMI (S1) channels

Resultant emissivity at first 9 GMI (S1) channels

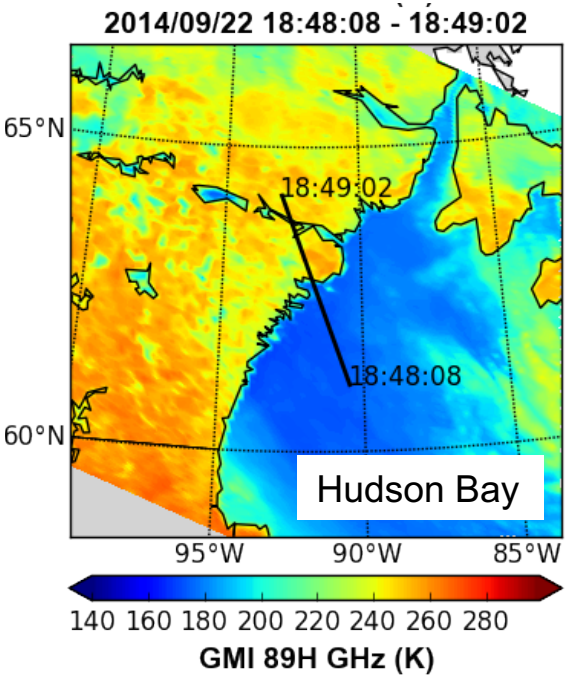

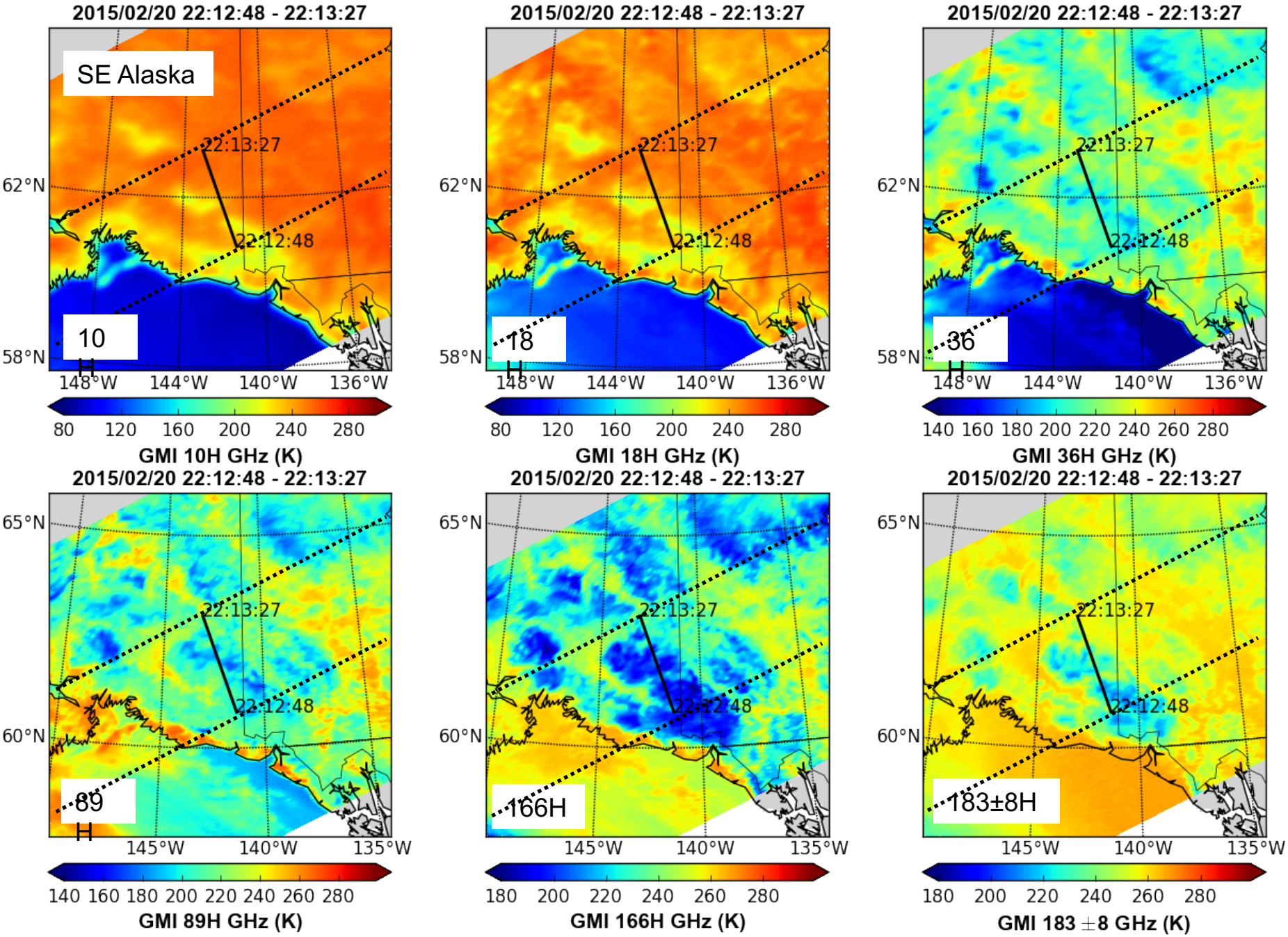
2015/02/20 22:12:48 - 22:13:27
SE Alaska
22:13:27
22:12:48
10 H
62°N
58°N
148°W
144°W
140°W
136°W
80 120 160 200 240 280
GMI 10H GHz (K)
2015/02/20 22:12:48 - 22:13:27
22:13:27
22:12:48
18 H
62°N
58°N
148°W
144°W
140°W
136°W
80 120 160 200 240 280
GMI 18H GHz (K)
2015/02/20 22:12:48 - 22:13:27
22:13:27
22:12:48
36 H
62°N
58°N
148°W
144°W
140°W
136°W
140 160 180 200 220 240 260 280
GMI 36H GHz (K)
2015/02/20 22:12:48 - 22:13:27
22:13:27
22:12:48
89 H
65°N
60°N
145°W
140°W
135°W
140 160 180 200 220 240 260 280
GMI 89H GHz (K)
2015/02/20 22:12:48 - 22:13:27
22:13:27
22:12:48
166H
65°N
60°N
145°W
140°W
135°W
180 200 220 240 260 280
GMI 166H GHz (K)
2015/02/20 22:12:48 - 22:13:27
22:13:27
22:12:48
183±8H
65°N
60°N
145°W
140°W
135°W
180 200 220 240 260 280
GMI 183 ±8 GHz (K)

GPM+CloudSat coincidence
20 February 2015
Alaska winter mountainous terrain

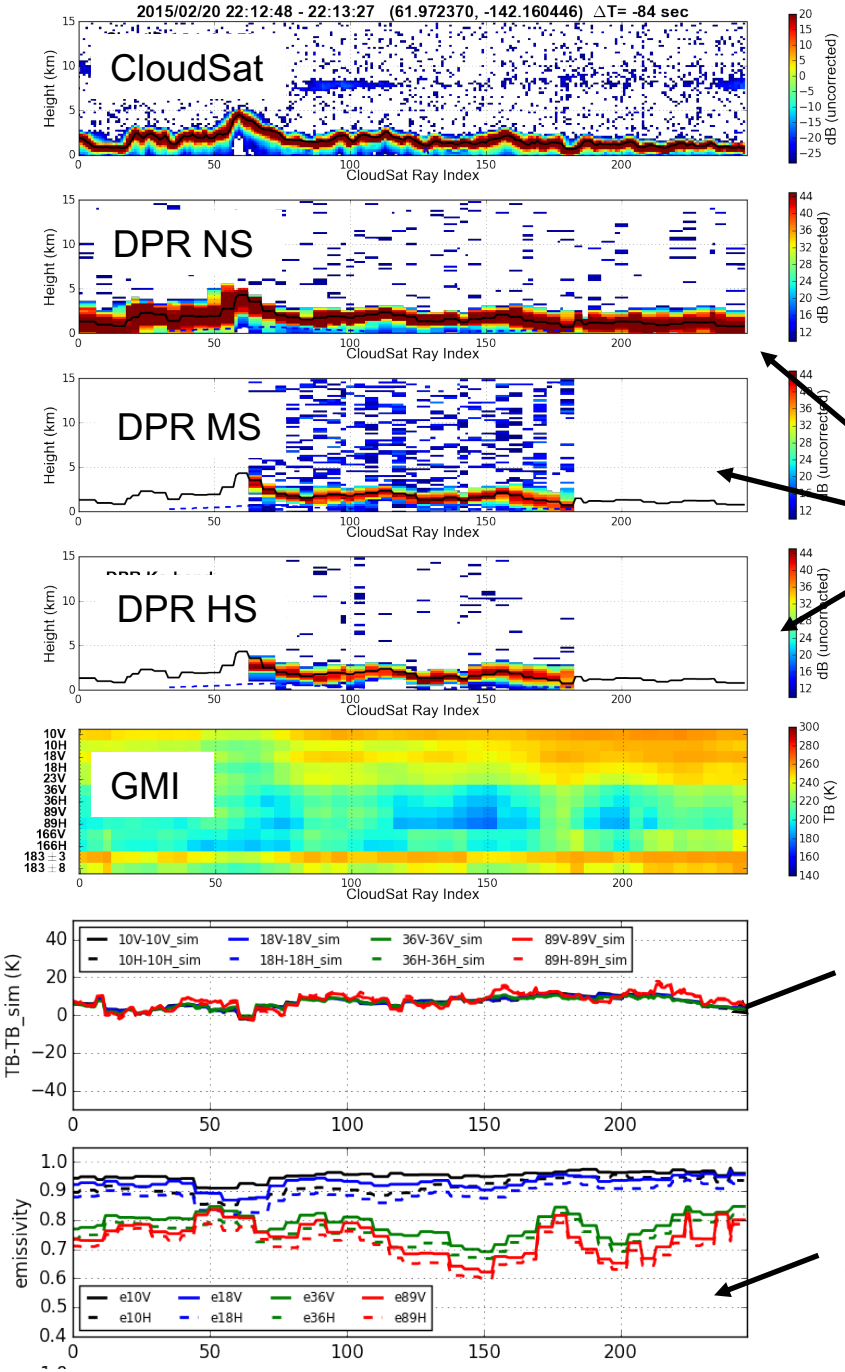

No clouds evident in all three DPR scans

Trace of all 13 GMI channels

Simulated TB difference (using ECMWF) within 10K across all 9 GMI (S1) channels

Resultant emissivity at first 9 GMI (S1) channels

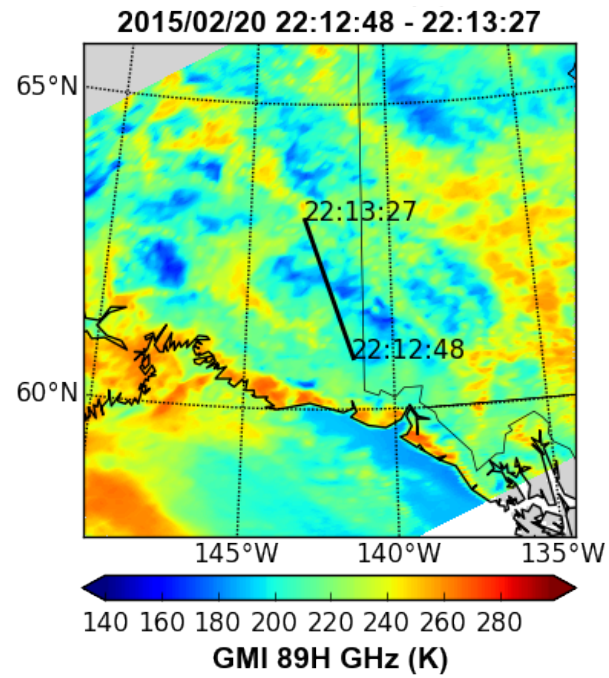

Extension to 166 GHz being examined for very dry cold scenes

Rain/Emissivity State Timeseries near a point: West of Lubbock, TX, US

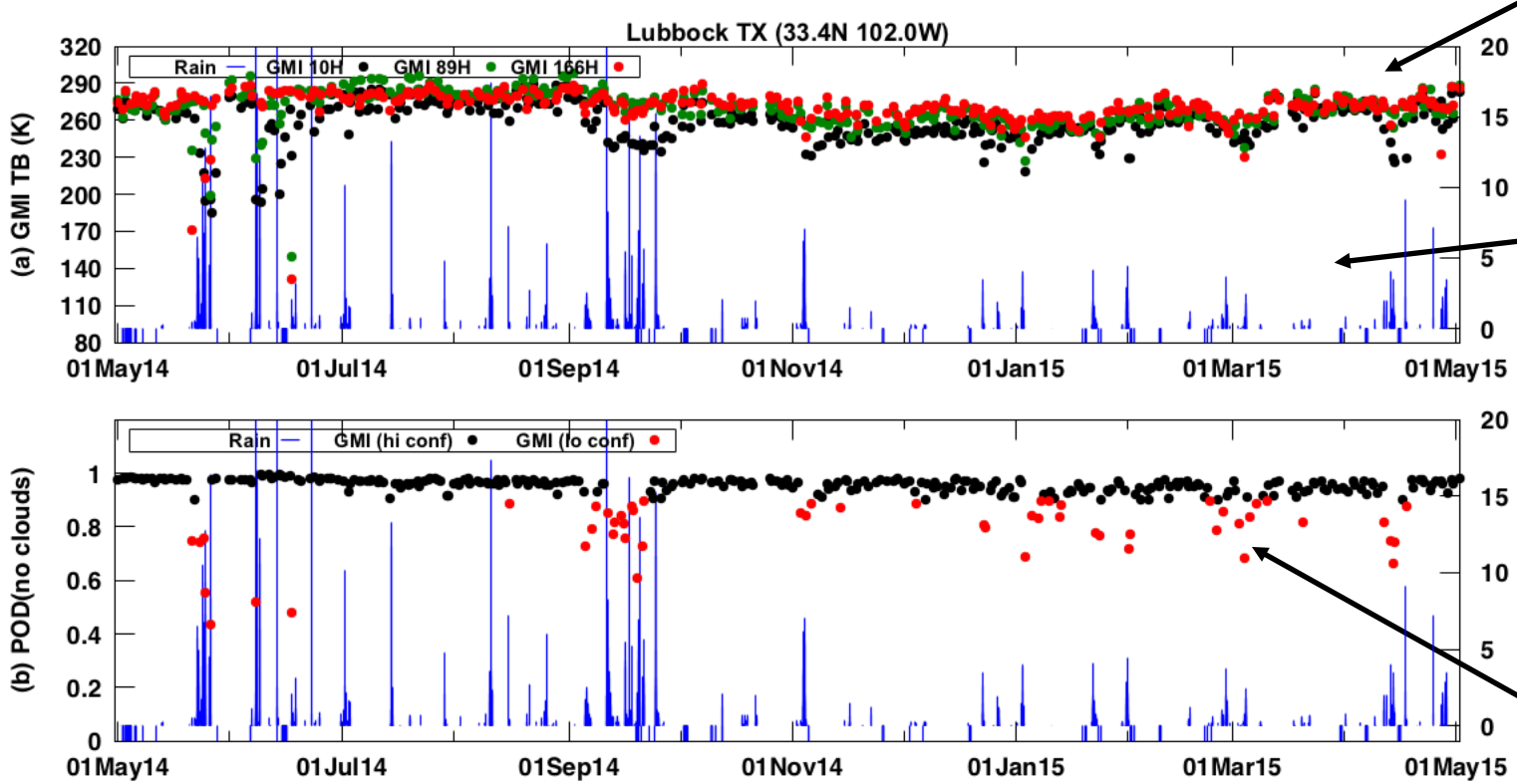

Observations
TB 10H
TB 89H
TB 166H

MRMS
1-hr rain

Discrimination
("no-cloud")
90% High
Confidence

Reduced
Confidence

12 months

1 May 2014 – 1 May 2015

Soil type and scrub-like vegetation exhibit rapid rain response and dry-down

Rain/Emissivity State Timeseries near a point: West of Lubbock, TX, US

Closed Circles= High Confidence, Open Circles= Reduced Confidence

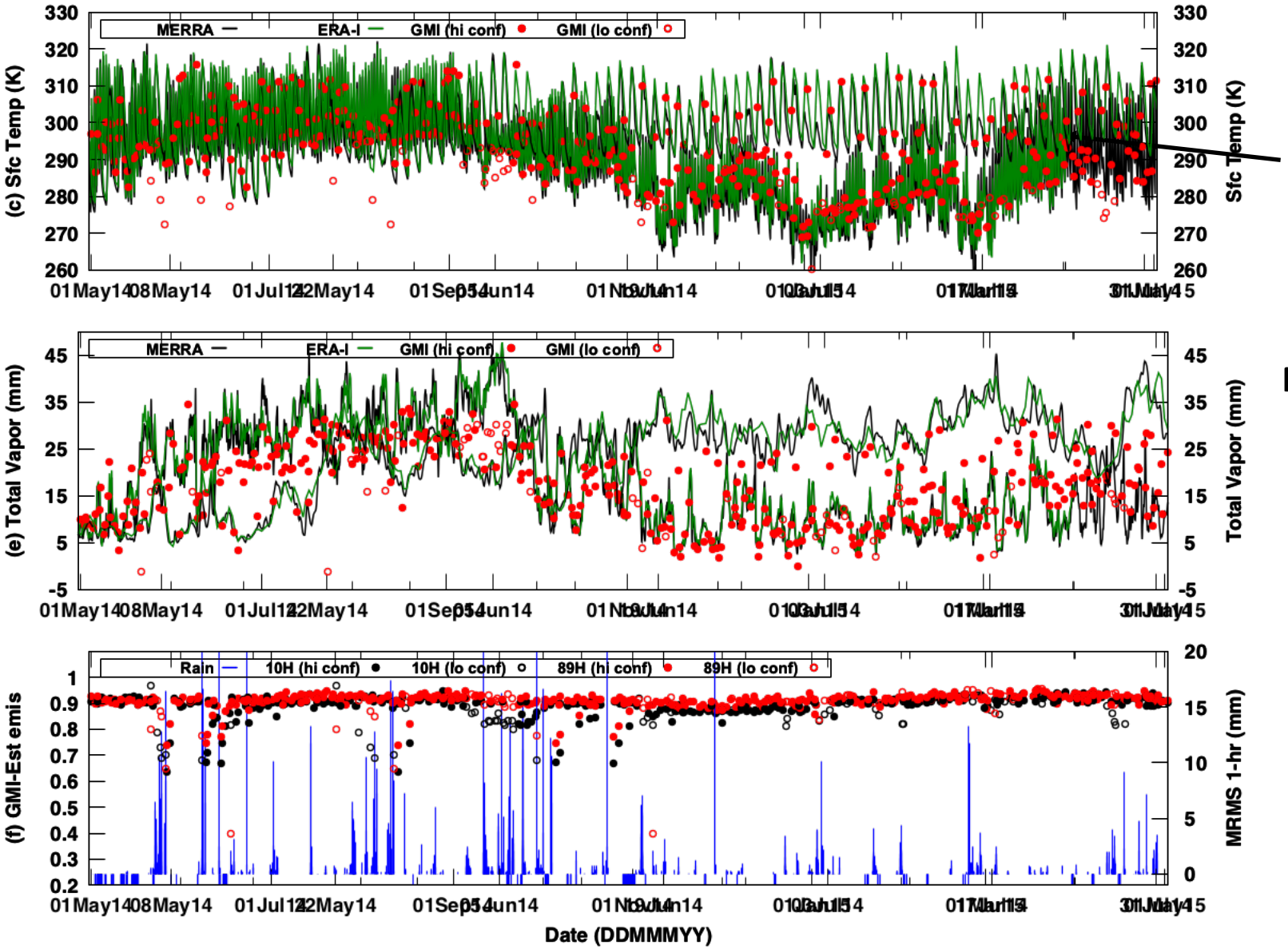

MERRA Ts
ERA-I Ts
Est. Ts

MERRA Tvap
ERA-I Tvap
Est. Tvap

Est. e10H
Est. e89H

MRMS
1-hr rain

Meghna River, Bangladesh, Seasonal Wetland ("Haor")

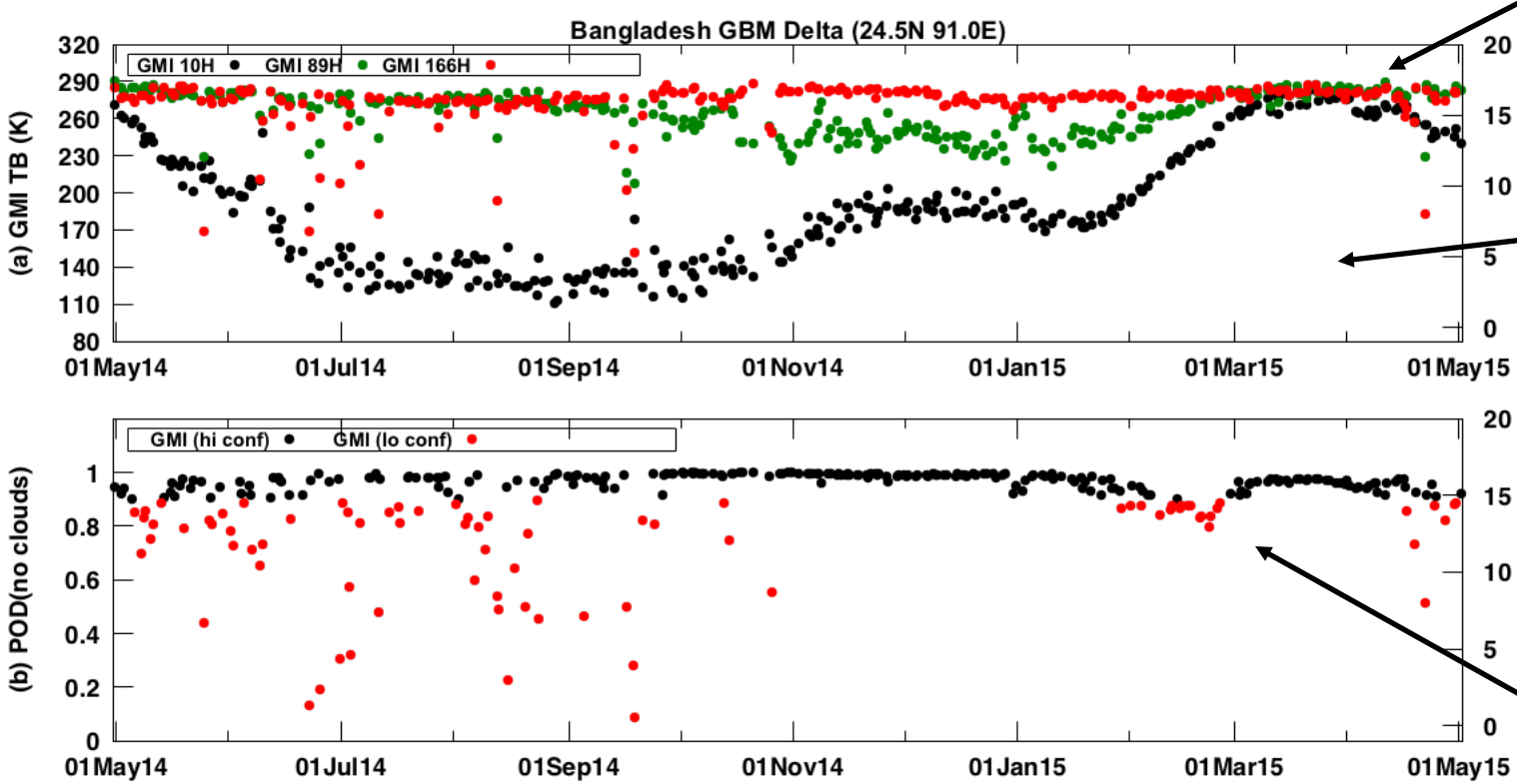

Observations

TB 10H

TB 89H

TB 166H

MRMS 1-hr rain

Discrimination ("no-cloud") 90% High Confidence

Reduced Confidence

12 months

1 May 2014 – 1 May 2015

Can also experience rapid emissivity change across inundated areas

Meghna River, Bangladesh, Seasonal Wetland ("Haor")

Closed Circles= High Confidence, Open Circles= Reduced Confidence

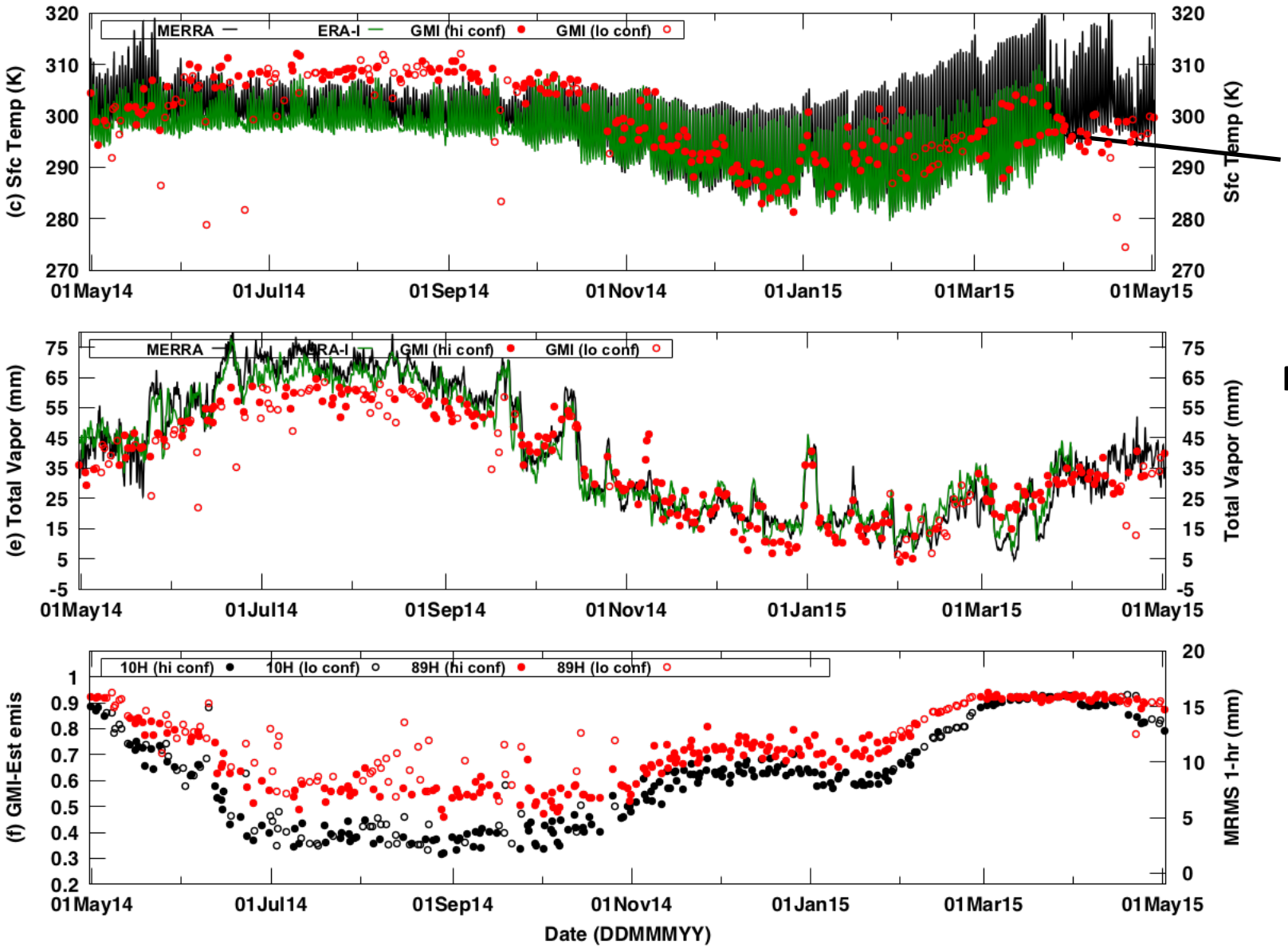

MERRA Ts
ERA-I Ts
Est. Ts

MERRA Tvap
ERA-I Tvap
Est. Tvap

Est. e10H
Est. e89H

MRMS
1-hr rain

Middle of Lake Superior, US/Canada

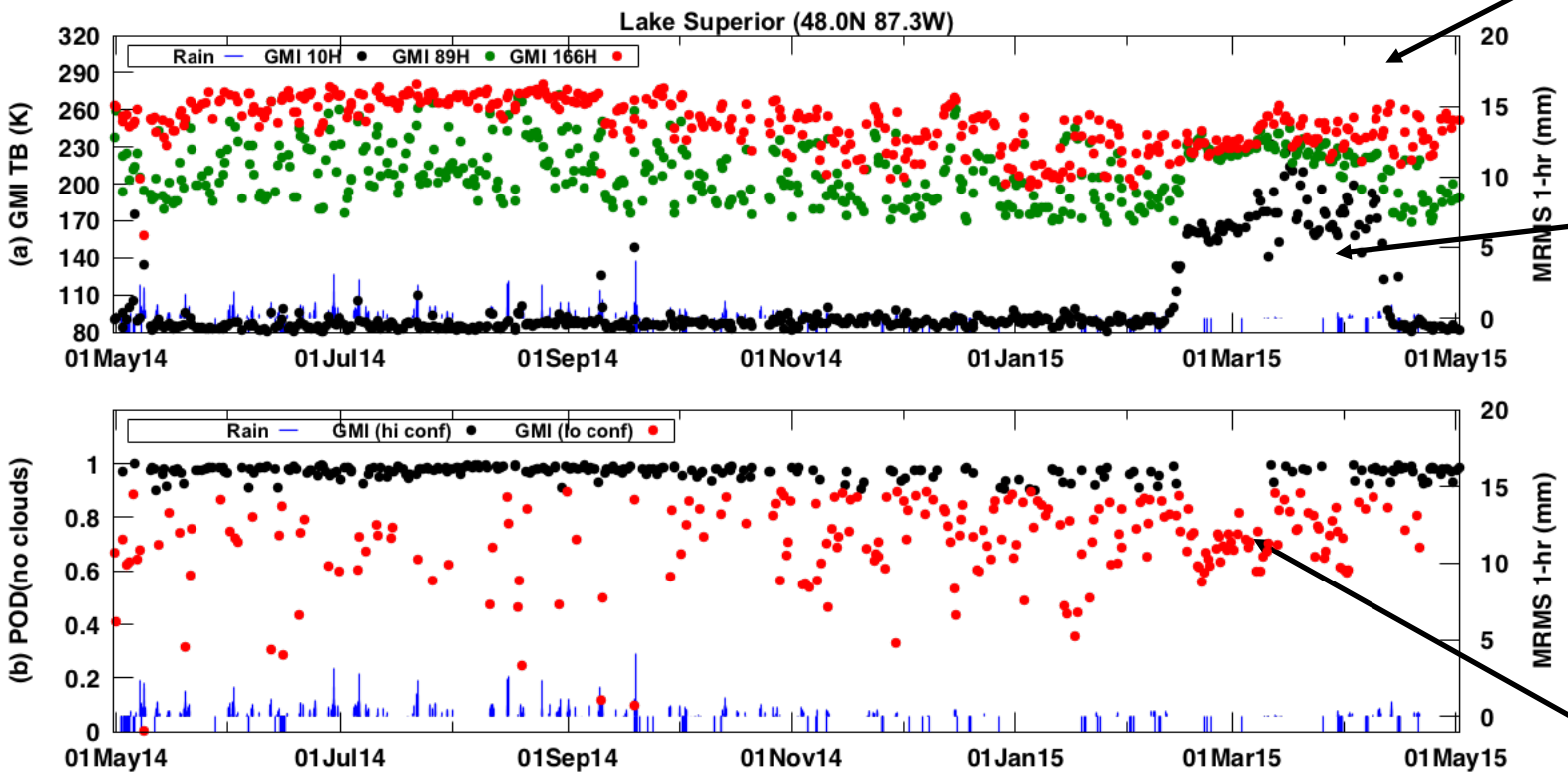

Observations

TB 10H

TB 89H

TB 166H

MRMS 1-hr rain

Discrimination ("no-cloud") 90% High Confidence

Reduced Confidence

12 months

1 May 2014 – 1 May 2015

Inland Water Throughout Freeze-Thaw Conditions

Middle of Lake Superior, US/Canada

Closed Circles= High Confidence, Open Circles= Reduced Confidence

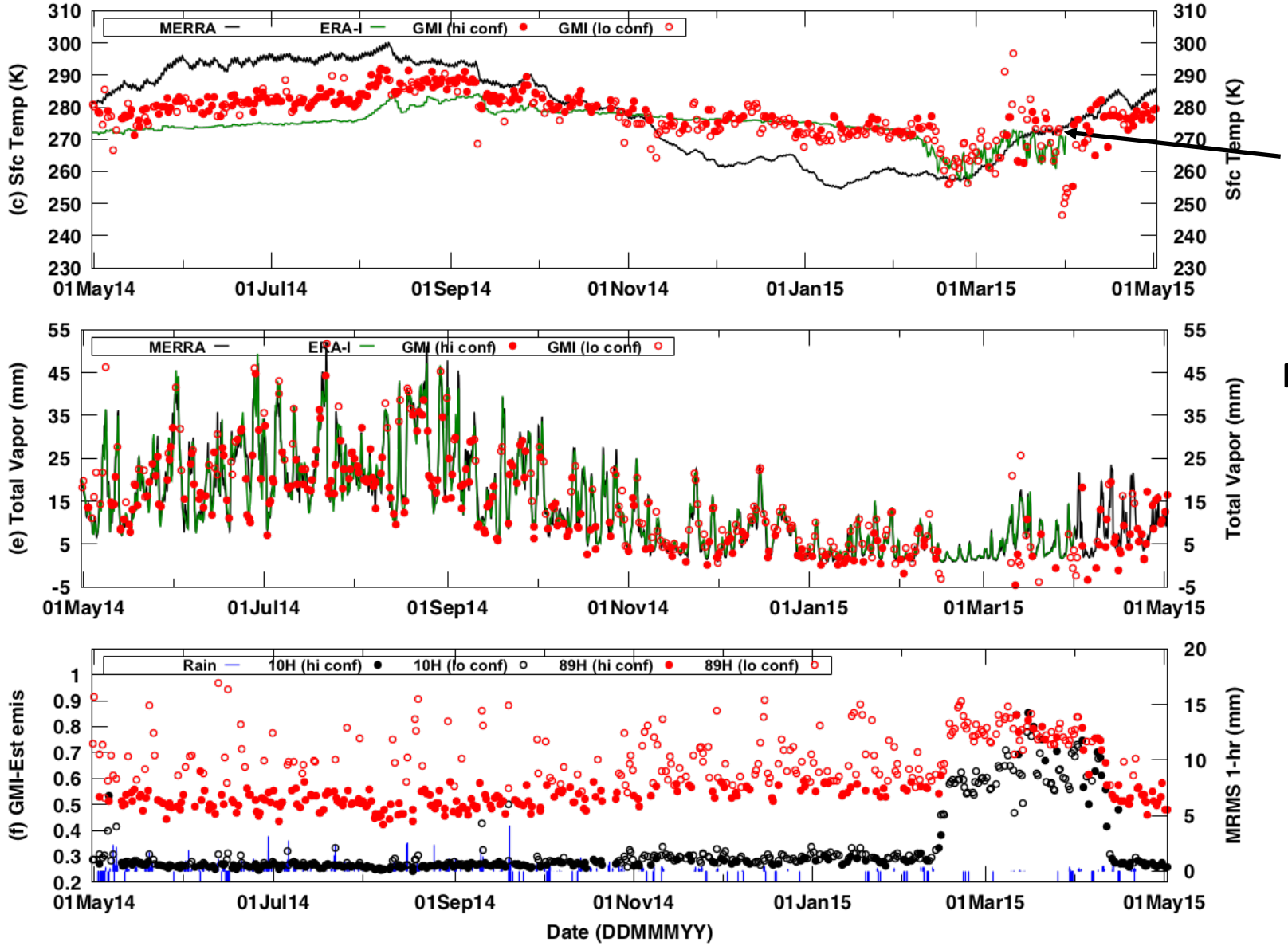

MERRA Ts
ERA-I Ts
Est. Ts

MERRA Tvap
ERA-I Tvap
Est. Tvap

Est. e10H
Est. e89H

MRMS
1-hr rain

Applicability to Database Search: Example from Over-Ocean Warm SST

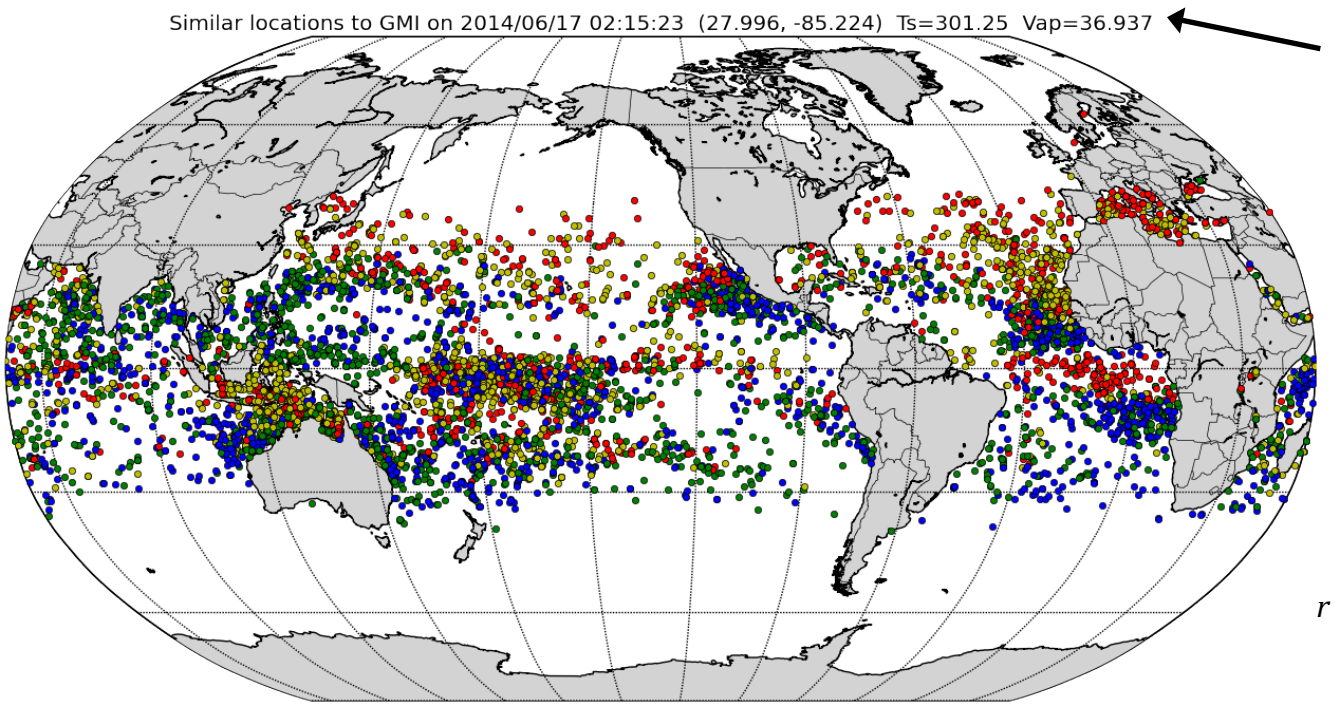

Gulf of Mexico
17 June 2014

DJF MAM
JJA SON

Search for "nearby" entries in leading EOF-space:

$$r = \sqrt{\frac{1}{N}\sum[(u^{obs} - u_i^{sim})/\sigma_i]^2} \quad N = 3$$

Throughout the process, the only time that latitude/longitude was ever consulted, was to plot the points on the map

Associated co-variability in emissivity

Associated co-variability in Tsfc and WV state variables

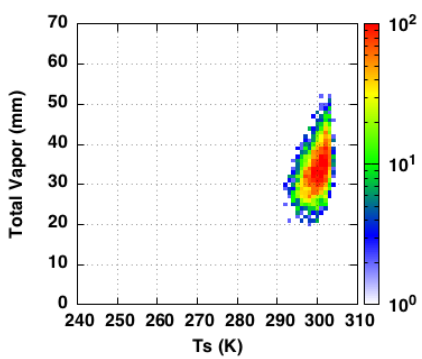

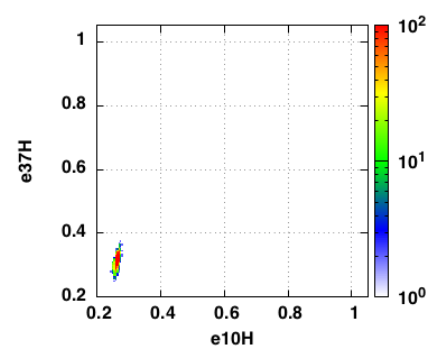

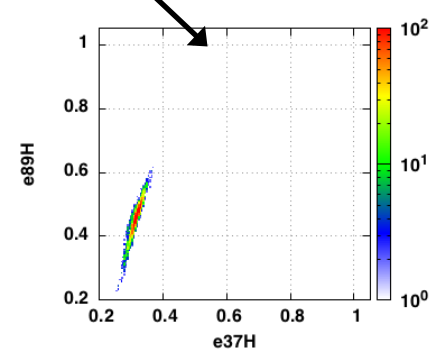

suggests possible alternate ways to index databases (transformation of variables)

Applicability to Database Search: Example from Midlatitude Inland Water

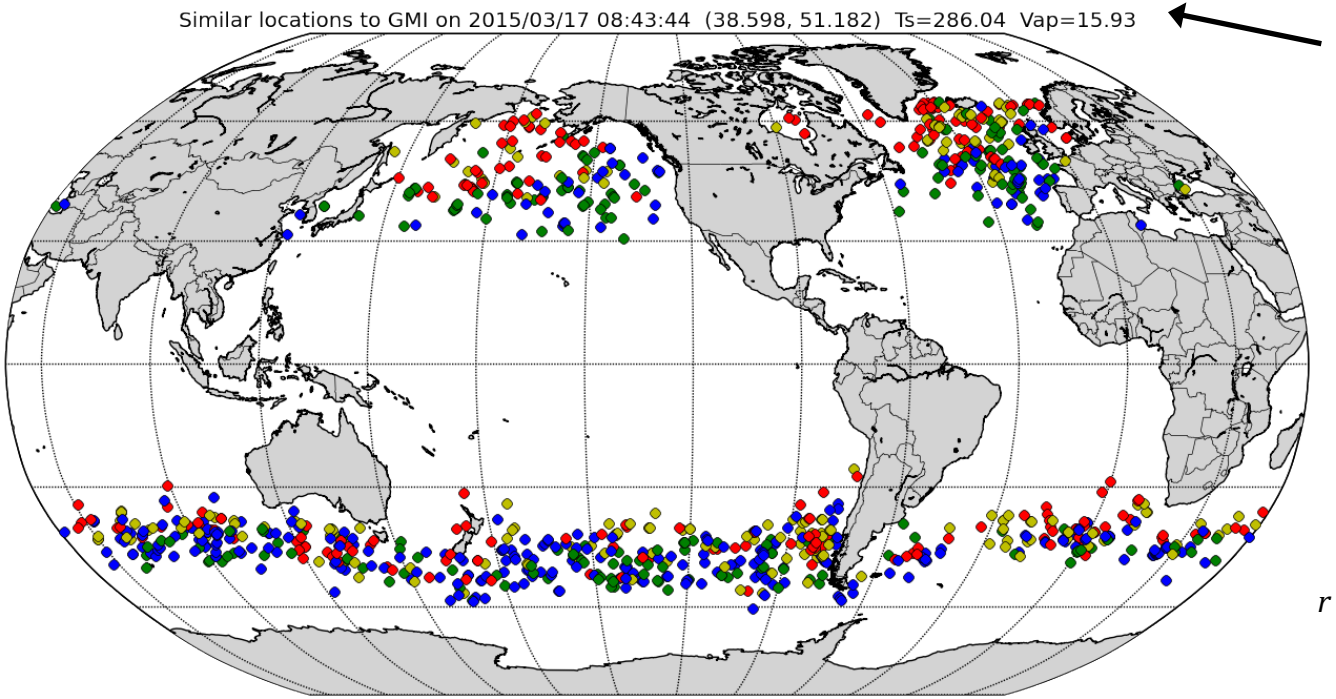

Center of the Caspian Sea 17 March 2015

DJF MAM
JJA SON

Search for "nearby" entries in leading EOF-space:

$$r = \sqrt{\frac{1}{N}\sum[(u^{obs} - u_i^{sim})/\sigma_i]^2} \quad N = 3$$

Throughout the process, the only time that latitude/longitude was ever consulted, was to plot the points on the map

Associated co-variability in emissivity

Associated co-variability in Tsfc and WV state variables

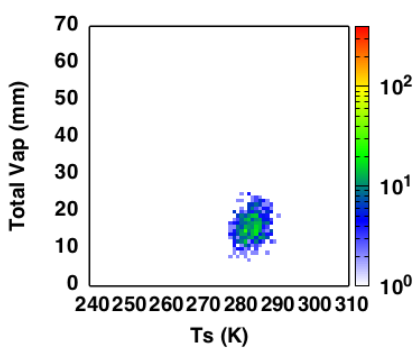

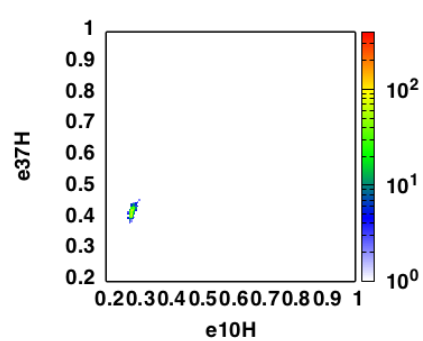

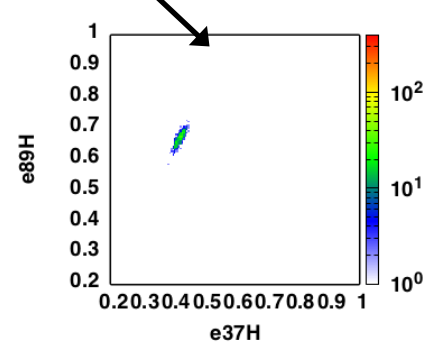

suggests possible alternate ways to index databases (transformation of variables)

Applicability to Database Search: Example from Bare Soil-Like, Daytime

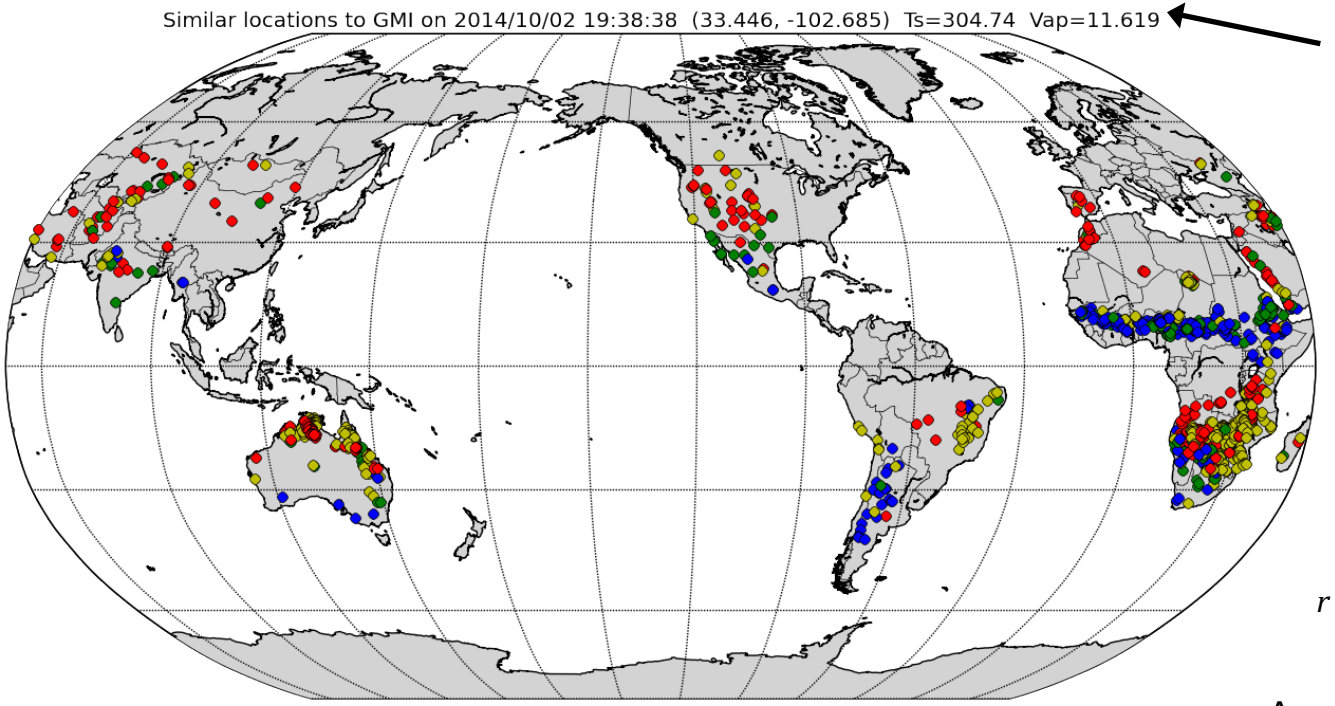

West Texas
2 October
2014

DJF MAM
JJA SON

Search for "nearby" entries in leading EOF-space:

$$r = \sqrt{\frac{1}{N}\sum[(u^{obs} - u_i^{sim})/\sigma_i]^2} \quad N = 3$$

Throughout the process, the only time that latitude/longitude was ever consulted, was to plot the points on the map

Associated co-variability in emissivity

Associated co-variability in Tsfc and WV state variables

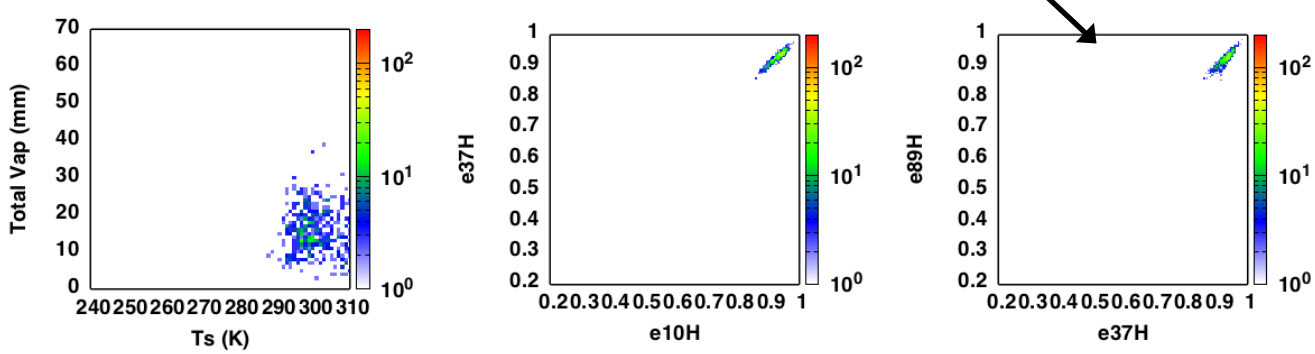

Applicability to Database Search: Snow Covered, Cold, Dry

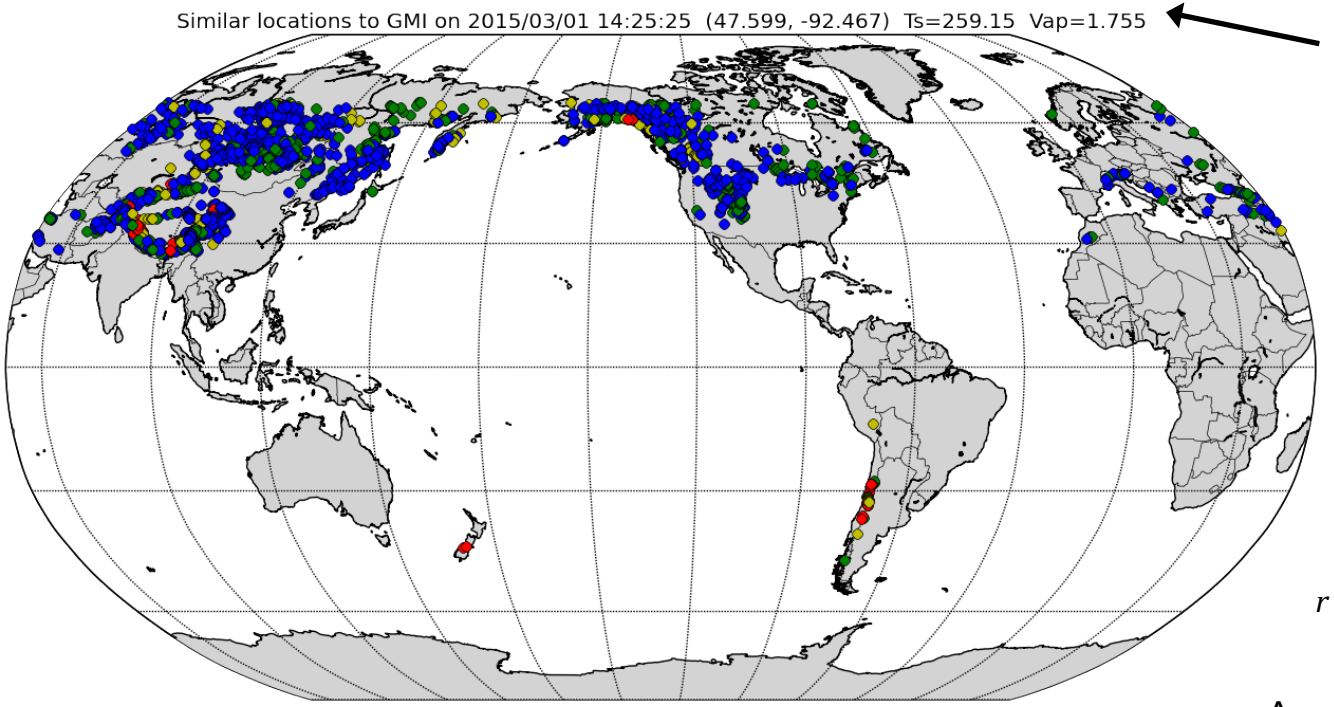

NE Minnesota, snow-covered 1 March 2015

DJF MAM
JJA SON

Search for "nearby" entries in leading EOF-space:

$$r = \sqrt{\frac{1}{N}\sum[(u^{obs} - u_i^{sim})/\sigma_i]^2} \quad N = 3$$

Throughout the process, the only time that latitude/longitude was ever consulted, was to plot the points on the map

Associated co-variability in emissivity

Associated co-variability in Tsfc and WV state variables

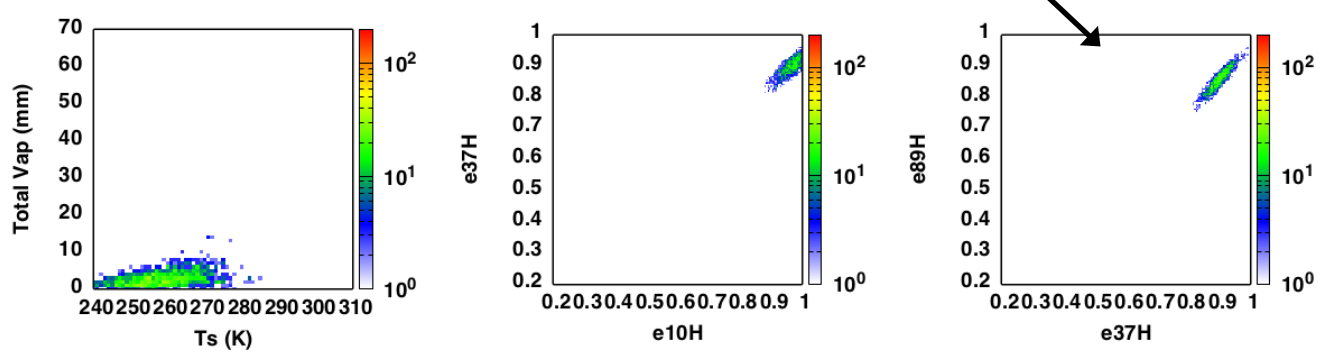

Satellite Remote Sensing of Snowfall – Active and Passive Sensing

Guosheng Liu

Florida State University

CloudSat Snowfall

- CloudSat Radar: 94 GHz
  From Ze to S

- *Present Study*:

  - six idealized shapes (Liu, 2004)
    - 3-,4-,5-,6-bullet rosettes
    - sector
    - dendrite
  - size distributions from field obs
    - Lo and Passarelli, 1982
    - Braham, 1990
  - random orientation
  - DDA simulations for backscattering

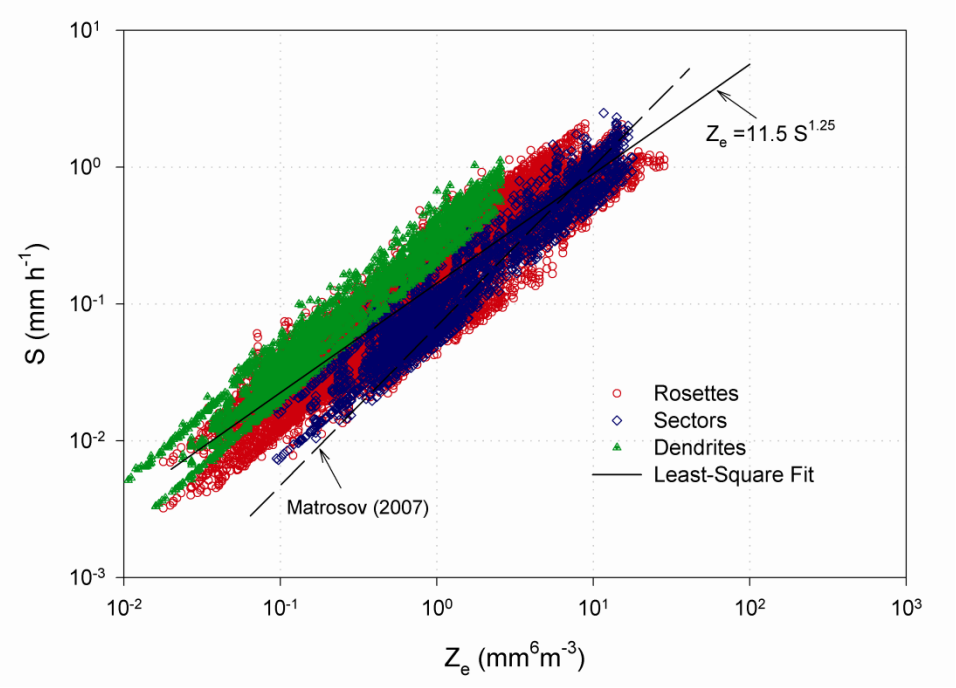

Liu, 2008

Active Sensing of Global Snowfall From CloudSat Data

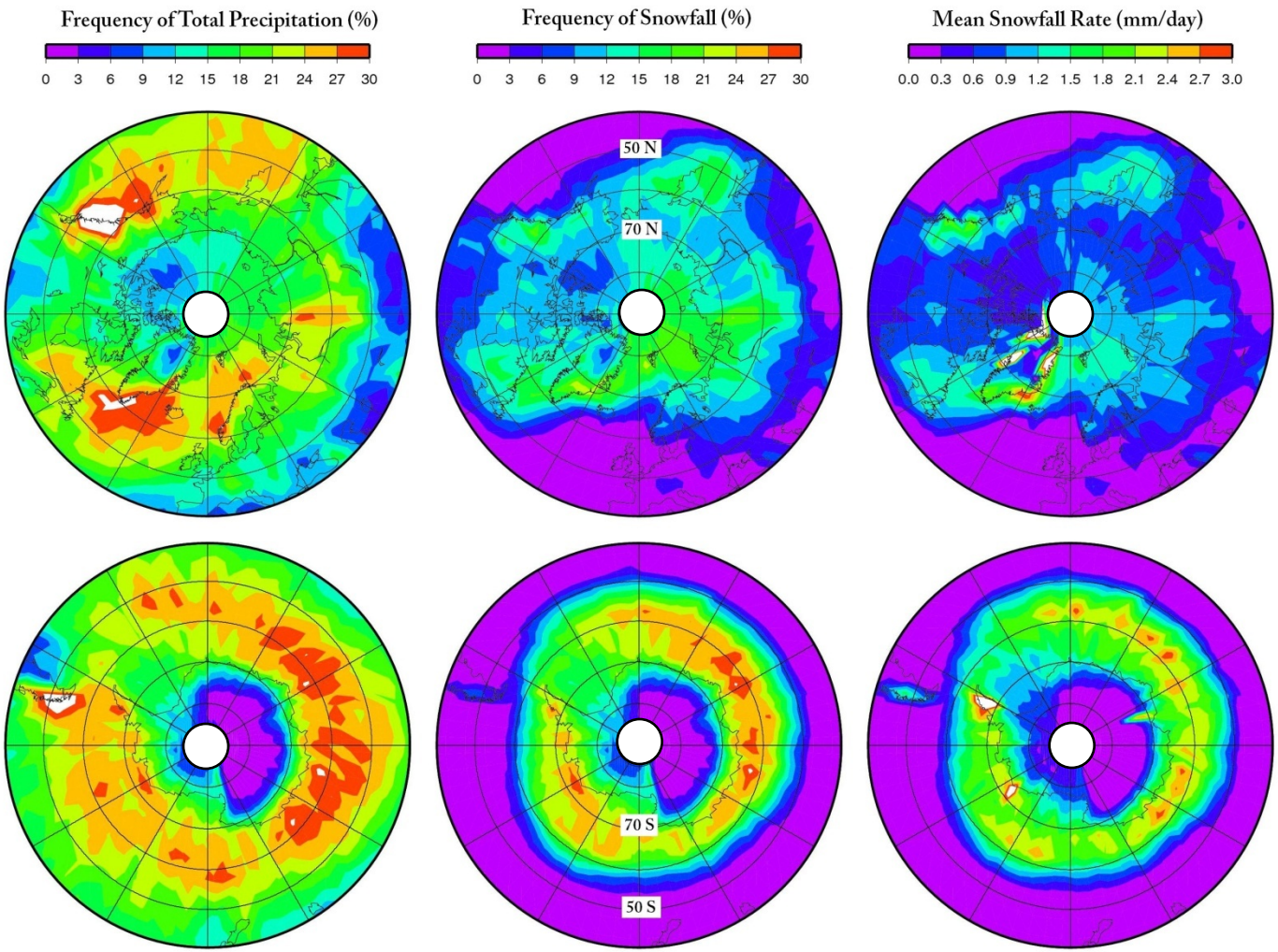

NP – 40°N

SP – 40°S

Rain+Snow Fraction

Snow Fraction

Mean Snowfall Rate

Reproduced using data from Liu (2008)

Snowfall "Climatology"

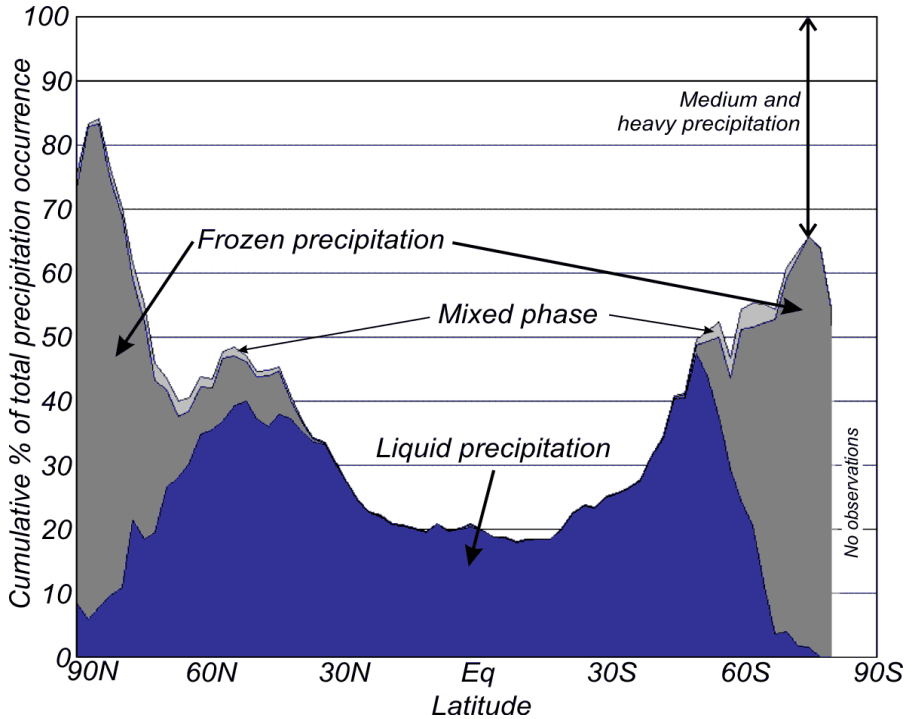

Occurrence Frequency and Snowfall rate, averaged over all observations of CloudSat from 2006 to 2010.

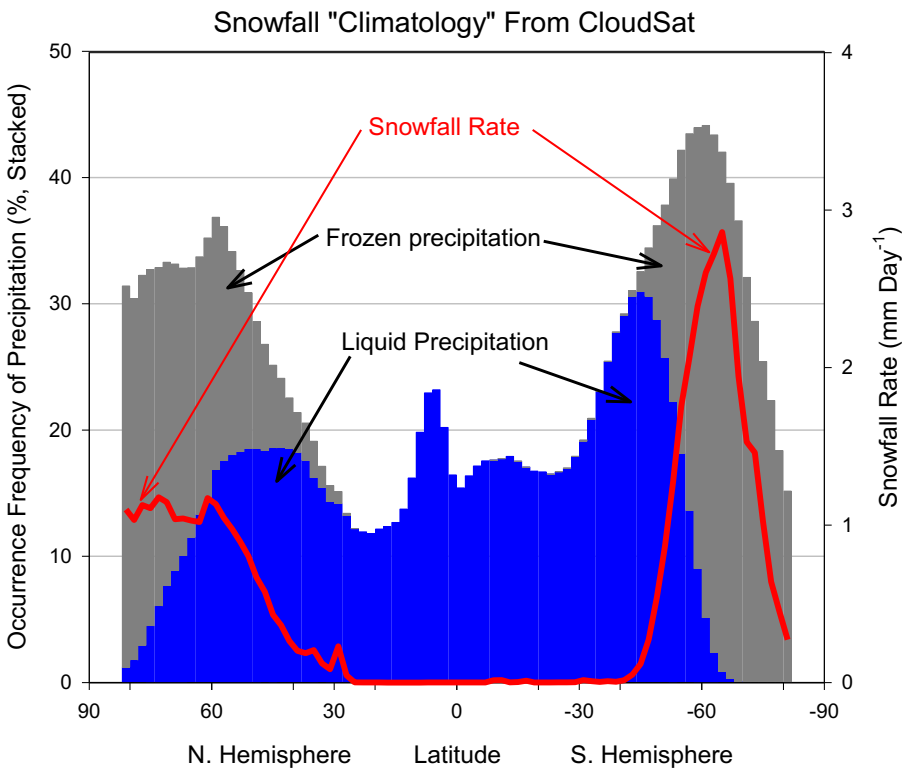

Mean Zonal occurrence of oceanic light precipitation (<1.0 mm/h) as a percentage of total precipitation occurrence, derived from COADS ship-borne data (1958-1991).

Use combined CloudSat/CPR and GPM/DPR as "truth"

CloudSat:DPR = 36:100

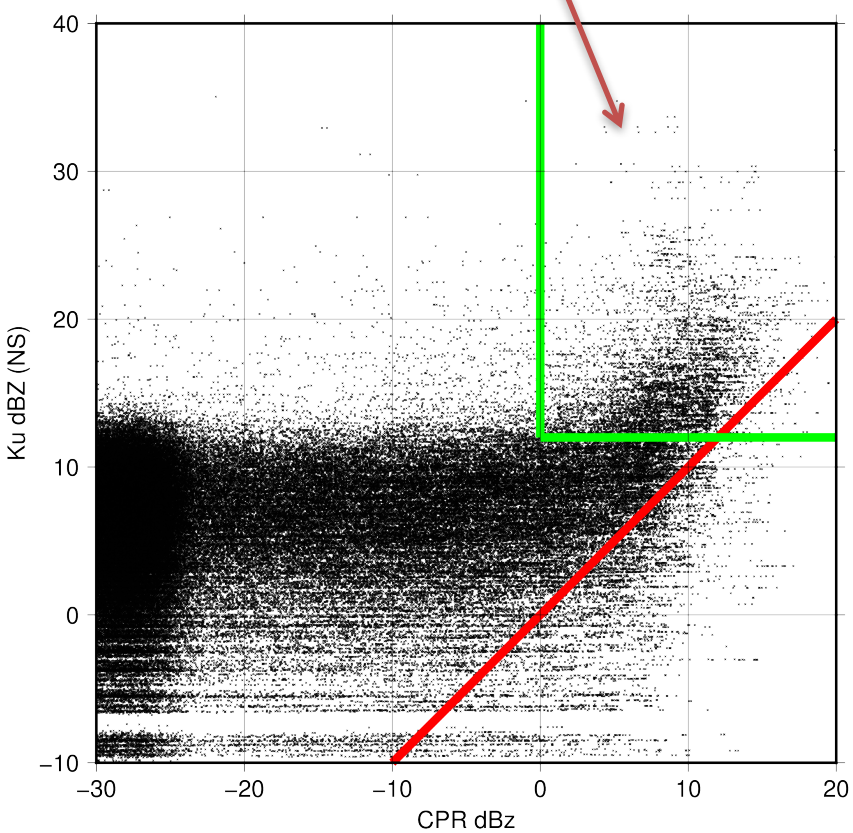

Based on collocated CloudSat/CPR - GPM/DPR data: Mar. 2014 – Dec. 2015

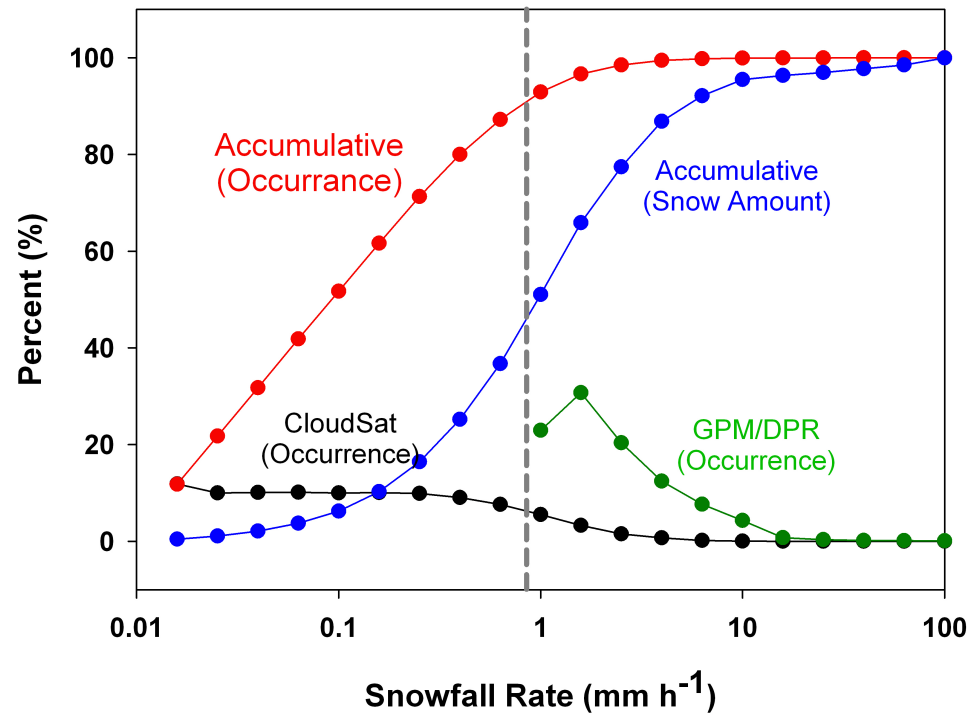

Use 2BCSATGPM dataset of Turk (2015)

DPR misses ~90% of snowfall pixels
~50% of snowfall amount

Passive Sensing
- vast amount of observational data so far

Satellites sensors w/ high-freq microwave observations An incomplete list

Satellite	*Sensor*	*Launch Date*
NOAA-15 (K)	AMSU-B	05/13/1998
NOAA-16 (L)	AMSU-B	09/21/2000
NOAA-17 (M)	AMSU-B	06/24/2002
NOAA-18 (N)	MHS	05/20/2005
NOAA-19 (N')	MHS	02/06/2009
MetOP-A	MHS	10/19/2006
MetOP-B	MHS	09/17/2012
DMSP F16	SSMIS	10/18/2003
DMSP F17	SSMIS	11/04/2006
DMSP F18	SSMIS	11/18/2009
NPP	ATMS	10/28/2011
GMP	GMI	02/27/2014

AMSU-B: Advanced Microwave Sounder Unit – B
MHS: Microwave Humidity Sounder
SSMIS: Special Sensor Microwave Imager Sounder
ATMS: Advanced Technology Microwave Sounder
GMI: GPM Microwave Imager

Difficulties

- Signal weak – except for graupels, snowflakes' signal is generally <50K for any channels
- Surface contamination – snow cover, etc
- Supercooled liquid in snowing clouds
- (similar to active sensing) Complication from particle shape, size distribution, etc.

One of the problems in detecting snowfall by passive MW observations – supercooled liquid

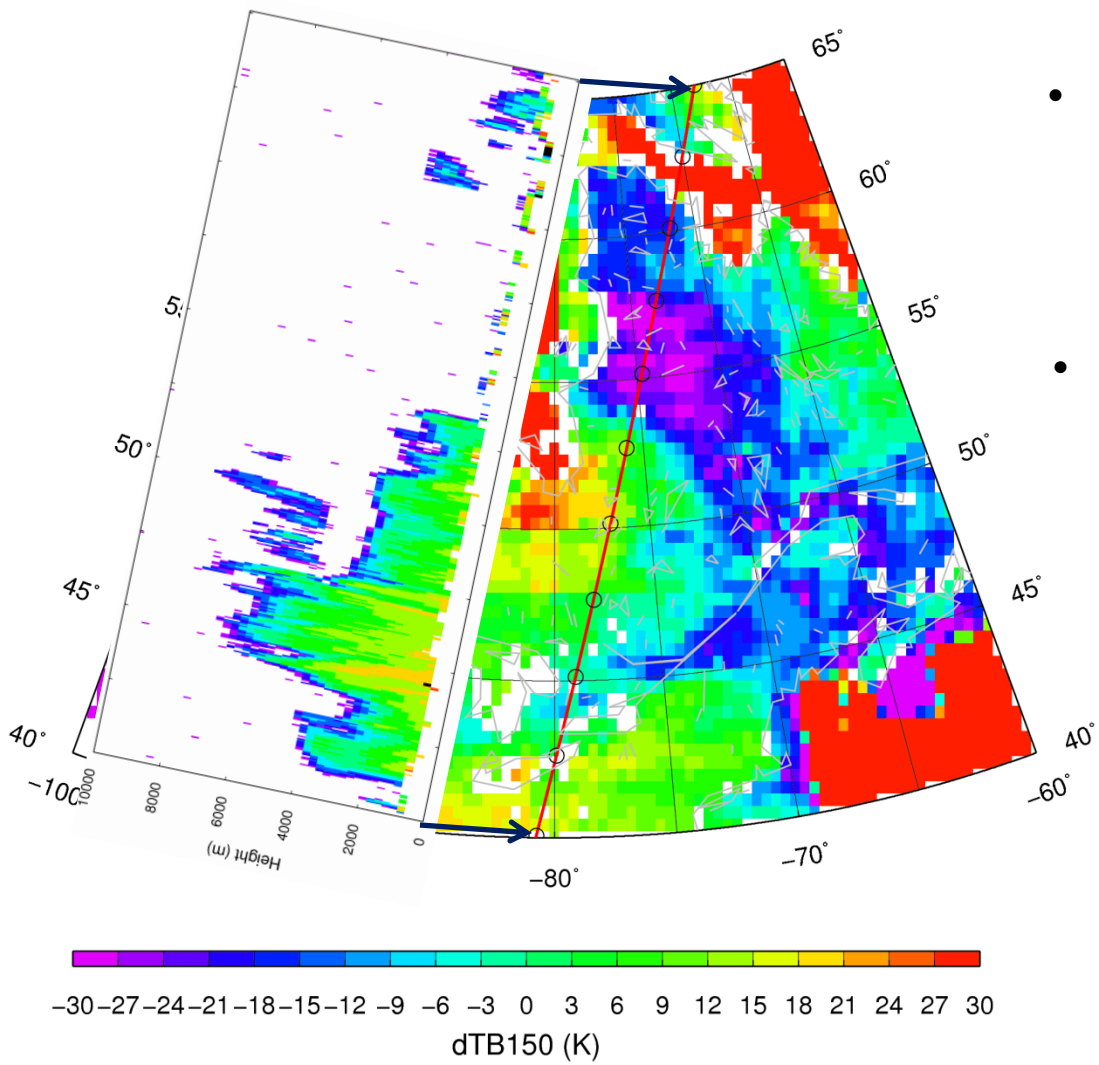

- The principle to detect snowfall from microwave obs. is to use TB decrease caused by ice-scattering
- Largest TB depression does NOT necessarily correspond to heavy snowfall
- Why ?

  Scattering by snowflakes competes with emission from cloud liquid.

Jan 22 2007 C3VP case w/CloudSat Over Pass ~ 0700UTC

Radar-Trained Passive Microwave Snowfall Algorithm (CloudSat-MHS Matchups)

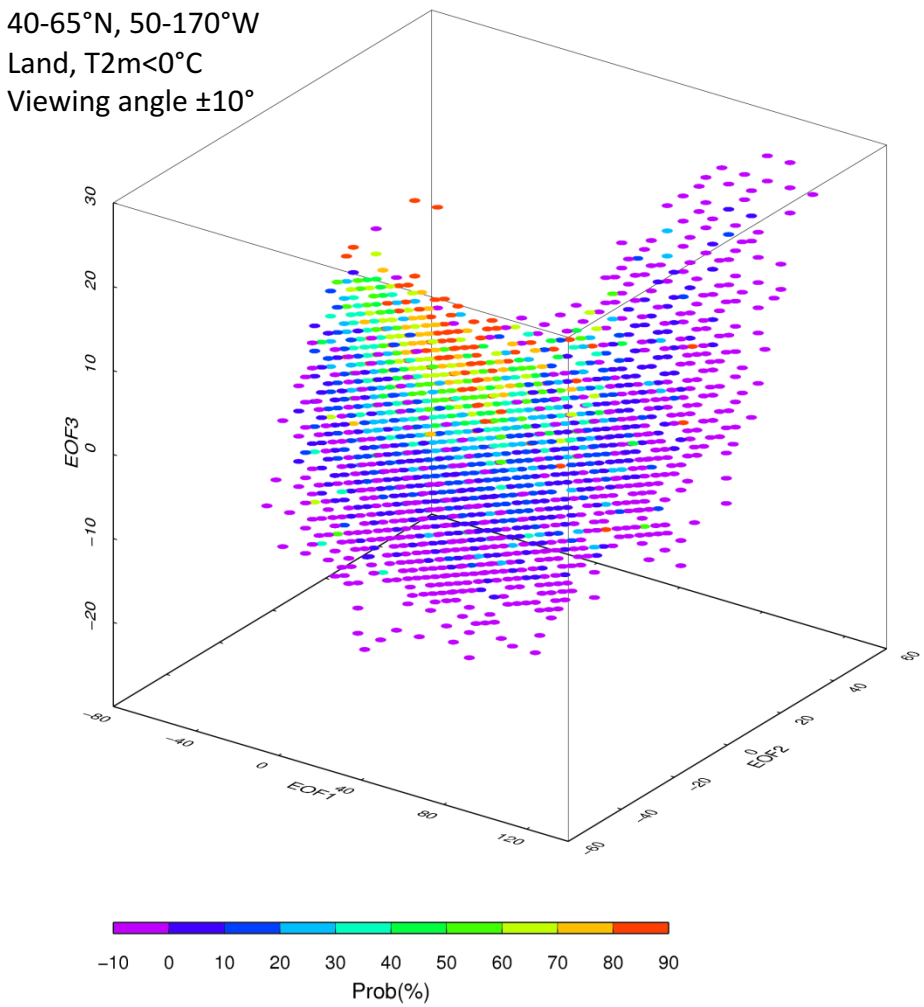

- EOF analysis to MHS data:
  - First 3 PCs – 88.6%, 8.2% and 2.1% of variances
  - PC3 had the best correlation Coeff to CloudSat reflectivity
- Lookup Table:
  - Project observed TBs to the first 3 PCs
  - In the 3-d EOF space, using MHS-CloudSat matchups, compute the probability of snowfall (CloudSat near-surface dBZe>-15)
  - Lookup tables for different MHS viewing angles
- Retrieve snowfall probability using the above lookup table; Use a Z-S relation, we can retrieve snowfall rate as well

Liu&Seo, 2013

Apply to C3VP Case – 2007.1.22

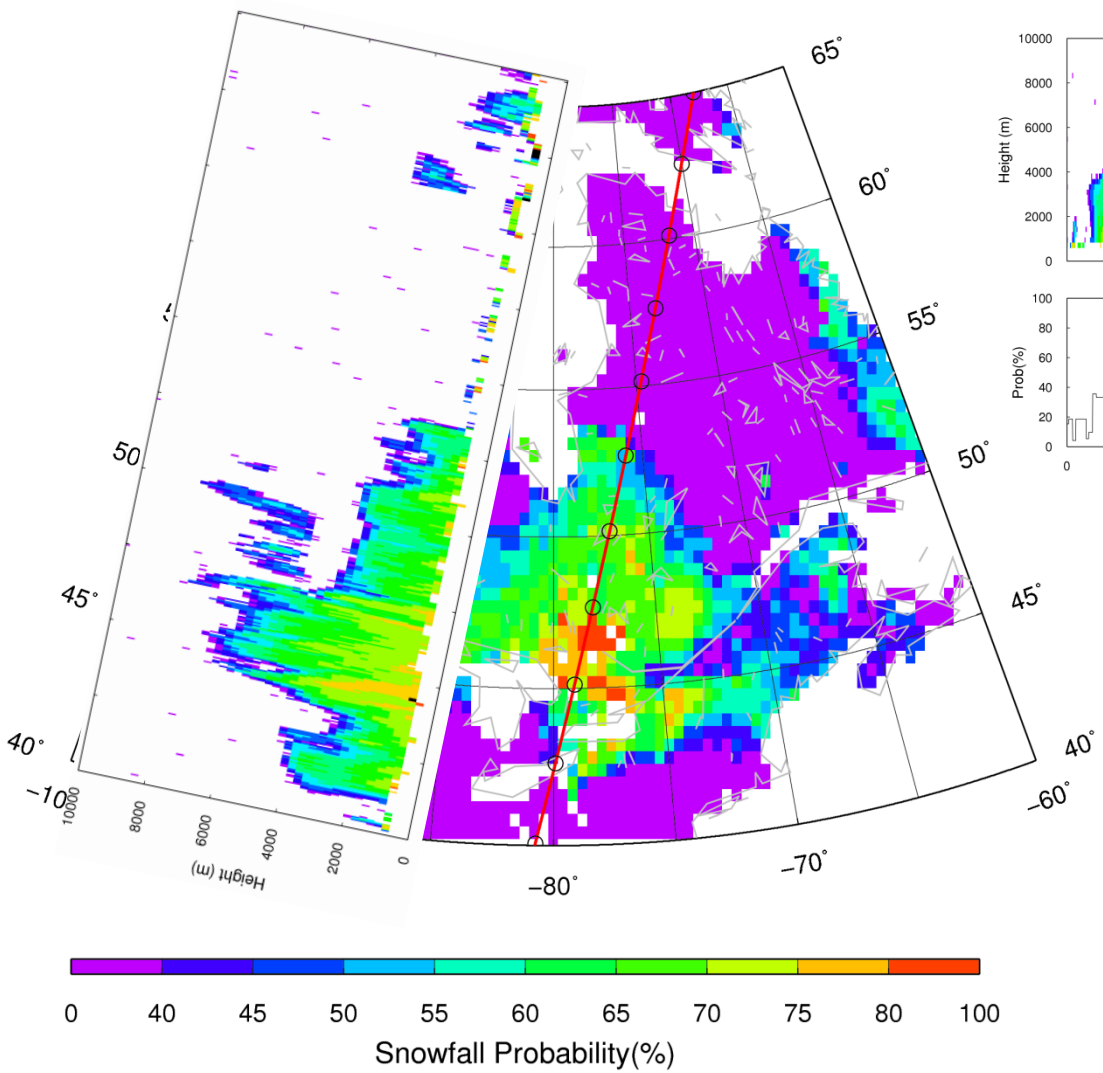

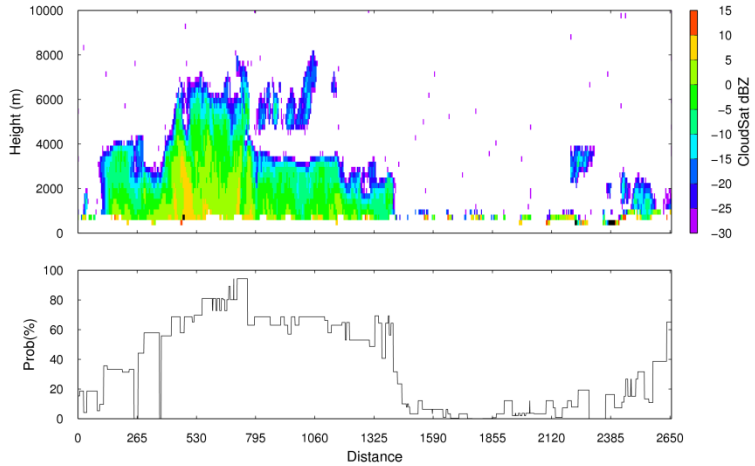

The look-up-table approach successfully identified snowfall area

CloudSat-Trained Passive Microwave Retrievals – U.S.

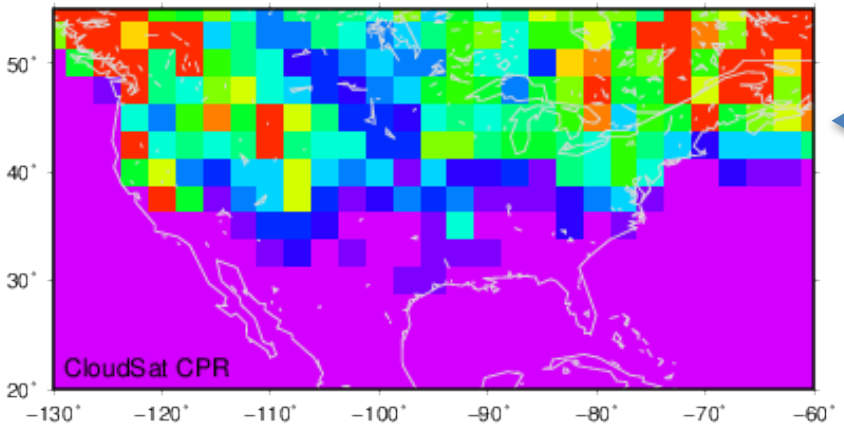

CloudSat
Averaged over 4 years
(2007-2010)

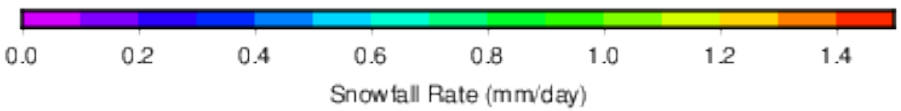

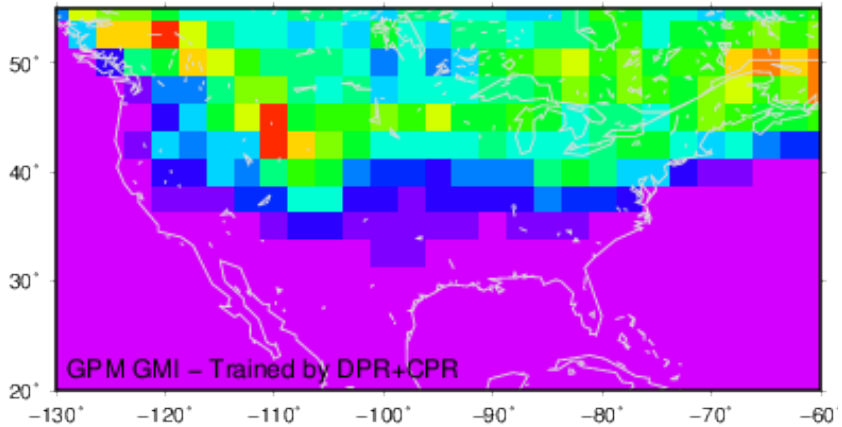

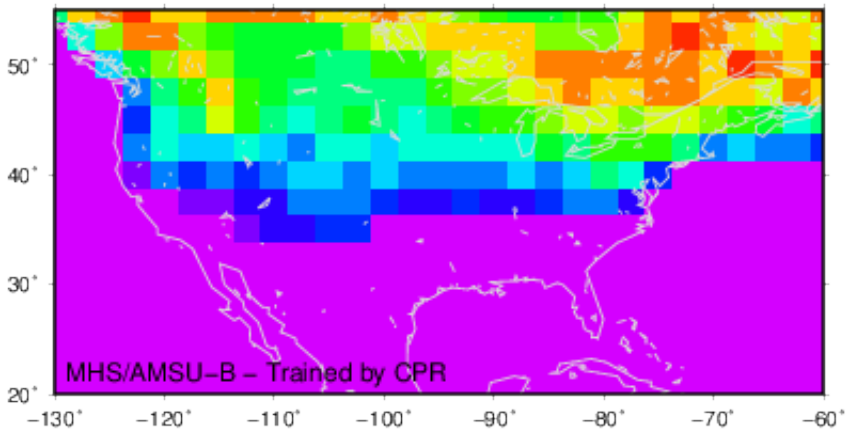

GMI
– trained by CloudSat&DPR
1 year (2014.04 – 2015.03)

AMSU-B/MHS (multi-satellites)
- trained by CloudSat
4 years (2007-2010)

CloudSat-Trained Passive Microwave Retrievals

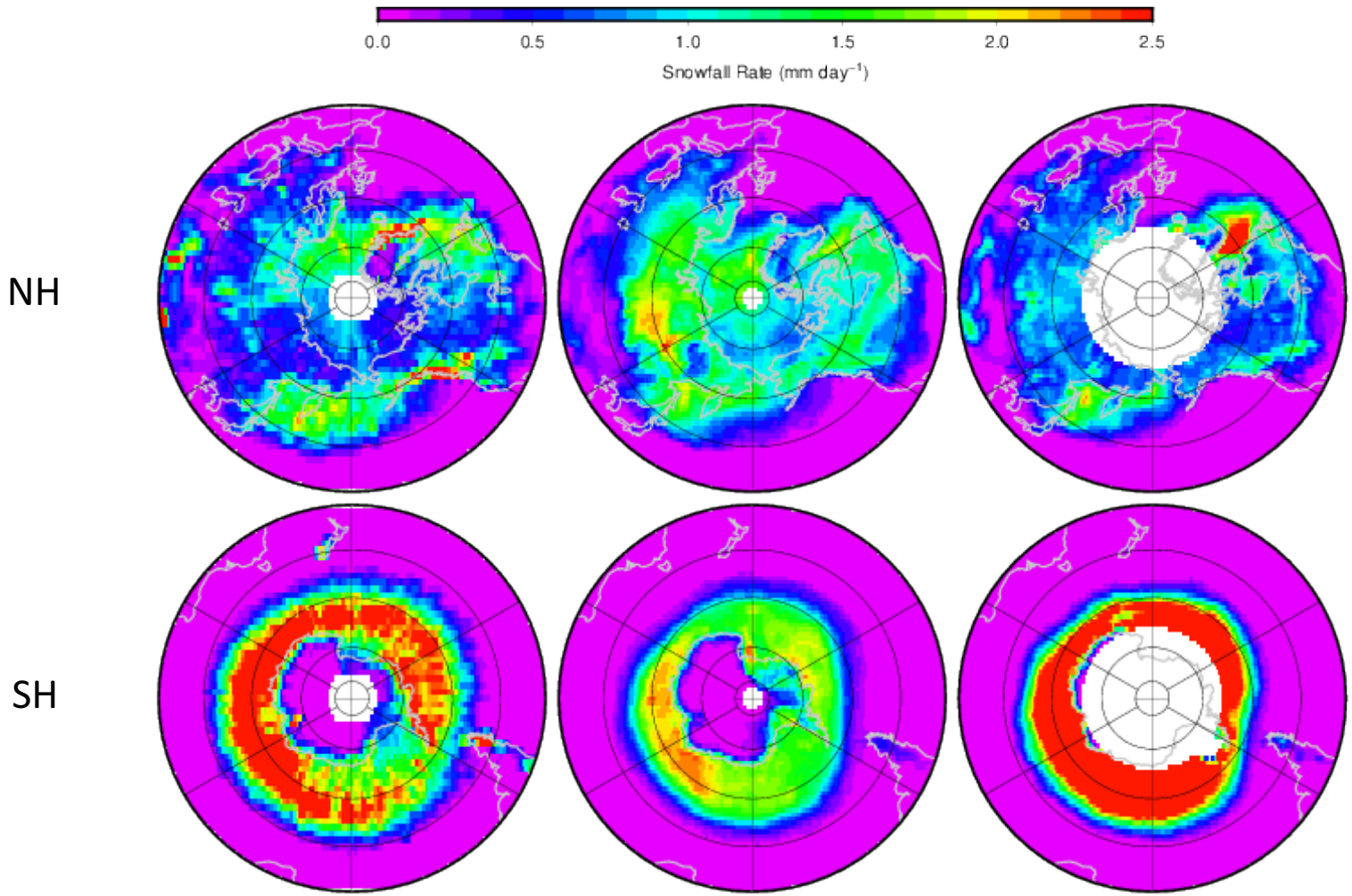

CloudSat
4 years (2007-2010)

AMSU-B/MHS
– trained by CloudSat
4 years (2007-2010)

GMI
– trained by CloudSat&DPR
1 year (2014.04-2015.03)

Concluding Remarks

- Separating rain and snow – a better algorithm than just using T or wet-bulb T; Lapse rate important
- A first of global snow “climatology” based on CloudSat, many issues/problems exist
- High-frequency microwave snowfall retrievals possible; need separated approach for land or ocean